

THESIS FOR THE DEGREE OF DOCTOR OF PHILOSOPHY

**Exploring binary mixtures
of protic ionic liquids**
Interactions, dynamics, and non-ideal behavior

Negin Yaghini



Department of Chemistry and Chemical Engineering

CHALMERS UNIVERSITY OF TECHNOLOGY

Gothenburg, Sweden 2016

Exploring binary mixtures of protic ionic liquids – Interactions, dynamics, and non-ideal behavior
Negin Yaghini

© Negin Yaghini, 2016.

ISBN 978-91-7597-419-4

Doktorsavhandlingar vid Chalmers tekniska högskola
Ny serie Nr 4100
ISSN 0346-718X

Department of Chemistry and Chemical Engineering
Chalmers University of Technology
SE-412 96 Gothenburg
Sweden
Telephone + 46 (0)31-772 1000

Cover illustration

My view of the puzzling task to thoroughly understand ionic liquid based binary mixtures. The chemical structures, and the Raman and infrared spectra are shown in each piece of the puzzle. The photo is used by the courtesy of Alexander Idström.

Printed at Chalmers Reproservice
Gothenburg, Sweden 2016

Exploring binary mixtures of protic ionic liquids – Interactions, dynamics, and non-ideal behavior

Negin Yaghini

Department of Chemistry and Chemical Engineering
Chalmers University of Technology

Abstract

Ionic liquids are organic salts that melt at low temperatures and provide a set of properties beneficial for diverse applications. These properties include good thermal stability, high ionic conductivity, low volatility and non-flammability. In this thesis protic ionic liquids have been at focus, which are of interest for use as electrolytes in next-generation proton exchange membrane fuel cells. The impact of the molecular structure of the ions as well as of the addition of a second compound on selected physicochemical properties has been investigated.

Imidazolium and ammonium based protic ionic liquids have been considered as possible proton conducting materials, whereas water, imidazole and ethylene glycol were chosen as neutral additives, all being a priori capable of forming hydrogen bonds. Transport properties like self-diffusion, ionic conductivity and viscosity have been thoroughly investigated, and the observed behavior explained in terms of established intermolecular interactions. These have been probed by ^1H NMR and vibrational (Raman and infrared) spectroscopy, used as powerful and complementary experimental tools.

Overall both self-diffusion and ionic conductivity increase upon addition of a second compound, but the extent of this increase very much depends on the molecular structure of the cation-anion pair in the ionic liquid, and the ability of the ions to establish hydrogen bonds. For example, in the case of the protic ionic liquid ethylimidazolium bis(trifluoromethanesulfonyl)imide ($\text{C}_2\text{HImTFSI}$) added water preferably interacts with the cation, while both cations and anions interact with added imidazole. These coordinations also results in very different phase changes and different mechanism of charge transport, with added imidazole promoting the Grotthuss mechanism of proton transfer as opposed to the case of added water. In a more hydrophilic protic ionic liquid like ethylimidazolium triflate (C_2HImTfO), however, water forms bonds with both cations and anions, and a local and fast proton exchange has been probed. Nevertheless, the choice of the added compound is not straightforward since not all required properties may be enhanced at once. For instance, while ethylene glycol affects ionic conductivity by a lesser extent it can provide a wider window of thermal stability.

The effect of confining an ionic liquid into nano-porous silica micro-particles has also been studied. The so called silica supported ionogels that we have considered can retain large volume fractions of the liquid and thus serve as support materials for electrolytes for use in fuel cell applications. Our results show that a strong interaction between the ammonium based protic ionic liquid (DEMA-OMs) and the pore walls of the silica nano-particles restricts the ionic mobility. As a solution to this effect the silica pore walls were functionalized with hydrophobic alkyl groups whereby a significant enhancement of the ionic conductivity was observed for the ionic liquid in the nano-sized pore domains. Our findings provide new useful insights for designing new electrolyte materials, the functionality of which will crucially depend on a careful selection of the ionic liquid, the added second compound and the surface chemistry of the support material. An optimal combination should be able to provide a fast and selective proton motion as required for use in fuel cells.

Keywords: protic ionic liquid, binary system, molecular interactions, nano-confinement

List of Publications

This thesis is based on the work presented in the following publications:

Paper I

Effect of Water on the Transport Properties of Protic and Aprotic Imidazolium Ionic Liquids – An Analysis of Self-diffusivity, Conductivity, and Proton Exchange Mechanism

Negin Yaghini, Lars Nordstierna and Anna Martinelli

Physical Chemistry Chemical Physics, **16**, 9266–9275 (2014)

Paper II

Effect of Water on the Local Structure and Phase Behavior of Imidazolium-Based Protic Ionic Liquids

Negin Yaghini, Jagath Pitawala, Aleksandar Matic, and

Anna Martinelli

The Journal of Physical Chemistry B, **119**, 1611–1622 (2015)

Paper III

Transport Properties, Local Coordination, and Thermal Stability of the Water/Diethylmethylammonium Methanesulfonate Binary System

Negin Yaghini, Mounesha N.Garaga, and Anna Martinelli

Fuel Cells, **1**, 46–54 (2016)

Paper IV

Local Coordination and Dynamics of a Protic Ammonium Based Ionic Liquid Immobilized in Nano-Porous Silica Micro-Particles Probed by Raman and NMR Spectroscopy

Mounesha N. Garaga, Michael Persson, Negin Yaghini, and

Anna Martinelli

Soft Matter, **12**, 2583–2592 (2016)

Paper V

Structural Origin of the Proton Mobility in a Protic Ionic Liquid/Imidazole Mixture. Insights from Computational and Experimental Results

Negin Yaghini, V. Gòmez Gonzàlez, L.M. Varela Cabo, and
Anna Martinelli

Submitted in revised form to Physical Chemistry Chemical Physics

Paper VI

Enhanced Ionic Mobility in Nanoporous Silica by Controlled Surface Interactions

Mounesha Nagendrchar Garaga, Luis Medina Aguilera, Negin Yaghini,
Aleksandar Matic, Michael Persson, and Anna Martinelli

Submitted to Small

Paper VII

Transport Properties and Thermal Stability of the Binary Mixture Ethylimidazolium Triflate/Ethylene glycol

Negin Yaghini and Anna Martinelli

In manuscript

Related publications not included in the thesis:

Chemical and Morphological Investigation of Cr(OH)₃ and Cr₂O₃ Nanoparticles

Adriano S. O. Gomes, Negin Yaghini, Nina Simic, Anna Martinelli and
Elisabet Ahlberg

In manuscript for Journal of Non-Crystalline Solids

My contribution to the appended papers

Paper I

I performed the experiments, the data analysis and wrote the primary versions of the manuscript.

Paper II

I performed the experiments, the majority of data analysis and wrote considerable parts of the manuscript.

Paper III

I performed the experiments, the data analysis and had the main responsibility in the writing process.

Paper IV

I prepared the silica-free samples, performed the diffusion and conductivity measurements for these samples and collaborated in the data analysis and in the writing process.

Paper V

I prepared the samples, performed the experiments, the data analysis (except the parts related to molecular dynamics simulations) and wrote the majority of the manuscript.

Paper VI

I performed the DSC and TGA experiments, analysed these data and participated in the discussion and writing of the whole paper.

Paper VII

I performed the experiments, the data analysis and was the main responsible for the writing process.

Contents

1	Introduction	1
1.1	Objectives	3
2	Background	5
2.1	Ionic liquids	5
2.1.1	History	6
2.1.2	General properties and applications	7
2.1.3	Synthesis	9
2.2	Protic ionic liquids	10
2.2.1	Application in fuel cells	11
2.3	Binary mixtures	13
2.4	Effects of nano-confinement	14
3	Theory	17
3.1	Self-diffusion	17
3.2	Conductivity	19
3.3	Ionicity	21
3.4	Proton transfer mechanism	23
3.5	Intermolecular forces	25

4	Characterization techniques	29
4.1	NMR spectroscopy	29
4.2	Diffusion NMR	30
4.3	Ionic conductivity	32
4.4	Density and viscosity measurements	33
4.5	Vibrational spectroscopy	33
4.5.1	Infrared spectroscopy	35
4.5.2	Attenuated total reflectance (ATR)	35
4.5.3	Raman scattering	37
4.5.4	The Raman spectrometer	38
4.6	Differential scanning calorimetry	39
4.7	Thermogravimetric analysis (TGA)	41
5	Results and discussions	43
5.1	Self-diffusion in ionic liquids	43
5.1.1	The effect of adding water	44
5.1.2	The effect of adding imidazole	45
5.2	Ionic conductivity	46
5.2.1	Adding water or ethylene glycol	48
5.3	Proton transfer	50
5.4	Density and viscosity	52
5.5	Intermolecular interactions	54
5.6	The effect of nano-confinement	59
6	Concluding remarks and future outlook	61
7	Acknowledgements	63
8	Appendix	i
8.1	The fuel cell technology	i
8.2	The proton exchange membrane fuel cell	ii
	Bibliography	v

List of Acronyms

IL	ionic liquid
PIL	protic ionic liquid
AIL	aprotic ionic liquid
PEMFC	proton exchange membrane fuel cell
EG	ethylene glycol
Im	imidazole
C₂HImTFSI	1-ethylimidazolium bis(trifluoromethanesulfonyl)imide
C₂HImTfO	1-ethylimidazolium trifluoromethanesulfonate
C₂C₁ImTFSI	1-ethyl-3-methylimidazolium bis(trifluoromethanesulfonyl)imide
C₂C₁ImTfO	1-ethyl-3-methylimidazolium trifluoromethanesulfonate
DEMA-OMs	diethylmethylammonium methanesulfonate
C₄C₁ImTFSI	1-butyl 3-methylimidazolium bis(trifluoromethanesulfonyl)imide
PYR₂₄TFSI	N-butyl-N-ethylpyrrolidinium bis(trifluoromethanesulfonyl)imide
PYR₁₄TFSI	N-butyl-N-methylpyrrolidinium bis(trifluoromethanesulfonyl)imide
PyrrHSO₄	pyrrolidinium hydrogen sulfate
PyrrCF₃COO	pyrrolidinium trifluoroacetate
PyrrTFSI	pyrrolidinium bis(trifluoromethanesulfonyl)imide
PFG-STE NMR	pulsed field gradient stimulated-echo nuclear magnetic resonance
¹H NMR	single pulse proton nuclear magnetic resonance
IR	infrared
QENS	quasi-elastic neutron scattering
ATR	attenuated total reflectance
CCD	charge coupled device
DMFC	direct methanol fuel cell
MCFC	molten carbonate fuel cell
SOFC	solid oxide fuel cell

Most of our grandfathers can not tell it anymore, and we can nothing but imagine how amazing it must have been to experience the first automobile driven by an internal-combustion engine. When speed and comfort were suddenly made available there were no thoughts about environmental issues. However, after decades of industrial and technological development in transport, we are now facing the problem of limited sources of fossil fuels, pollution, and global warming. According to recent reports the transport sector accounts for about 30% of the whole CO₂ emission in developed countries [1]. The awareness of these issues motivates the development of cleaner technologies for the supply of power, such as the fuel cell and the Li-ion battery, as well as the use of renewable energy sources, for example biofuels obtained from lignocellulose or vegetable oils.

For applications in the transport sector, the fuel cell has superior attributes like high efficiency, zero emission, and clean reaction products. Despite this advantages, the fuel cell has not yet reached a broad market, the major barrier being the production cost, which is mainly related to the catalyst and the proton conducting membrane. Moreover, the availability of an infrastructure for hydrogen supply is still an issue even in well-developed countries. Therefore to facilitate a wider implementation of the fuel cell, cheaper and better performing fuel cell components need to be developed.

To date the archetypical electrolyte used in a proton exchange membrane fuel cell (PEMFC) consists in an acidic aqueous solution retained by a polymer membrane. The ionic conductivity of the membrane is therefore severely dependent on humidity and is limited to below 80 °C due to dehydration. In view of this limitation, anhydrous electrolytes would be appropriate alternatives to conventional aqueous electrolytes. Protic ionic liquids have recently attracted considerable attention as anhydrous electrolytes for fuel cell applications due to their low volatility, high thermal stability, and high ionic density [2]. The knowledge of these emerging materials however is still at an early stage, and a lot remains to be understood on for instance the relation between the properties of the ionic liquid and the molecular structure of the constituent ions. For instance, different anions can establish hydrogen bonds of different nature and strength with the same cation thus resulting in different transport properties [3]. As the understanding of how the molecular structure determines macroscopic properties has improved, a desire to tune these to suit specific applications has also emerged. A very recent approach is by addition of a second miscible component like water [4] or a thermally more stable compound such as imidazole. In the specific context of protic ionic liquids for fuel cell applications, the ability of this second compound to form hydrogen bonds is key. Another important issue is whether a second compound can enhance the transport properties and the thermal stability of a protic ionic liquid. Moreover, the observed effects should be explained on a molecular level as an input for future materials design. An additional challenge related to applications is the transfer of the desired properties from the liquid to the solid-like state, as needed for use in an open system such as the fuel cell that requires non-leaking materials.

In this context, this thesis focuses on exploring the structure-property relation in protic ionic liquids (PILs) as neat materials or in binary mixtures. We first focused on water/PIL mixtures, limiting the study to selected imidazolium based protic ionic liquids of the TFSI and the TfO anions that, compared to other anions, provide relatively low viscosities. Properties of relevance for fuel cell applications such as conductivity, ionic mobility and phase behaviour have been investigated and tentatively explained in terms of intermolecular interactions. Based on the achieved results, we extended our study to other binary systems based

on a second compound with a higher thermal stability than water. The selected compounds were imidazole and ethylene glycol, almost unexplored in the context of protic ionic liquids. Finally, the effect on the transport properties and the local coordination upon confinement of a protic ionic liquid in silica based hybrid materials was also investigated.

1.1 Objectives

The main objective of this thesis was to provide a molecular-level understanding on how the addition of a second compound affects the transport and thermal properties of protic ionic liquids. In particular, the diffusivity, the local proton exchange, and the ionic conductivity were investigated by pulsed field gradient nuclear magnetic resonance (PFG-NMR) and impedance measurements, respectively. In addition, the nature of intermolecular interactions established between ions or between an ion and the added neutral compound, with particular attention to hydrogen bonds, was investigated by employing single pulse proton nuclear magnetic resonance (^1H NMR) and vibrational spectroscopy (Raman and infrared). As a complement to these spectroscopic techniques, calorimetric and thermogravimetric measurements were performed to study the phase behavior and the thermal stability of the investigated materials.

The whole work presented in this thesis pivots around ionic liquids, emerging materials that consist of only ions, have a low melting temperature and display high ionic conductivities. These properties, however, depend on the structure of the constituent ions and on the interactions established between them. Coulombic attraction, hydrogen bonds and dispersion forces are the main intermolecular forces in ionic liquids, the balance between which forces varies for different ionic liquids. It is crucial to understand these interactions on a molecular level, in particular when certain properties are sought for specific applications. One approach to tune intermolecular interactions is to change the molecular structure of the ions. Another is to manipulate these interactions by mixing the ionic liquid with a second compound. This chapter gives a brief introduction of the history, synthesis, and types of ionic liquids known so far. It also explains the concept of a binary mixture based on a protic ionic liquid and a neutral molecule like water or imidazole, as well as the mechanisms of proton transfer and the effects of nanoconfinement.

2.1 Ionic liquids

Ionic liquids are defined as organic salts that melt at temperatures below 100 °C [5]. These low melting temperatures (compare with table

salt, or NaCl, that melts at 801 °C) arise from the asymmetric and bulky structure of the ions that prevents efficient packing and thus the formation of a crystalline solid. Ionic liquids also show very large liquid windows, high thermal and electrochemical stability and low volatility, properties that make them appropriate for use in electrochemical applications. Although ionic liquids have been known for more than a century [6], attention to them boosted in the last 10-20 years (Figure 2.1) when non-volatility was highlighted as key property. During the past decade the number of possible applications identified for ionic liquids has increased, and now include solar cells, Li-ion batteries, dissolution of cellulose, electrodeposition, tribology and catalysis [5], to mention a few.

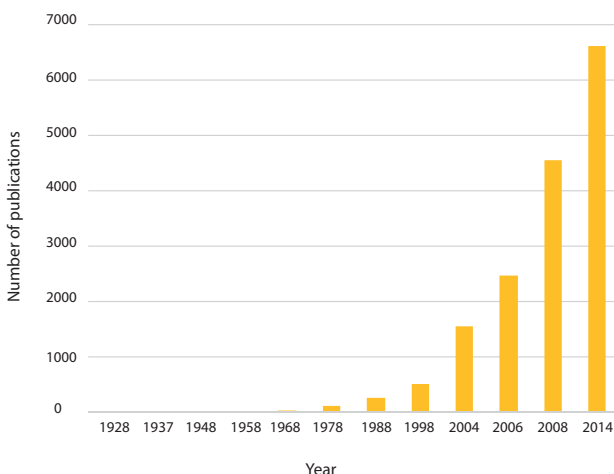


Figure 2.1: Number of documents published over the years as obtained from a search on Scopus using the term "ionic liquid" as a keyword.

2.1.1 History

The first ionic liquid reported in literature was ethylammonium nitrate (EAN) synthesized by Paul Walden in 1914 [6] with a melting point of 12 °C (Figure 2.2). In 1930 the application of a pyridinium based molten salt was reported for cellulose dissolution at temperatures above 130 °C [5]. Later on, in 1976, imidazolium and pyridinium based ionic

liquids started to attract attention as electrolytes for use in batteries and fuel cells due to their high ionic conductivity, fluidity and negligible vapor pressure [7].

A typical ionic liquid consists of a bulky cation, usually an imidazolium, pyridinium, pyrrolidinium, or ammonium [8], and an organic or inorganic anion, such as BF_4^- , PF_6^- , CF_3SO_3^- and $(\text{CF}_3\text{SO}_2)_2\text{N}^-$ (Figure 2.3). Up to date, three generations of room temperature ionic liquids have been invented. The first generation ionic liquids, based on the AlCl_4^- anion, were synthesized in the 1990's, had melting points below 50 °C, and high conductivity and fluidity [9, 10], but were unstable in the presence of water. The second generation of ionic liquids consisted of fluorinated anions such as BF_4^- and PF_6^- , were more stable in water and had higher conductivities at room temperature [7, 11]. Applications such as ionic catalyst solution in hydrogenation and as solvents in liquid-liquid extraction have been reported for this class of ionic liquids [12, 13]. The third generation is that of protic ionic liquids (sometimes referred to in the literature as PILs), which have exchangeable protons on the cation and have been targeted as suitable electrolytes for fuel cell applications [14].

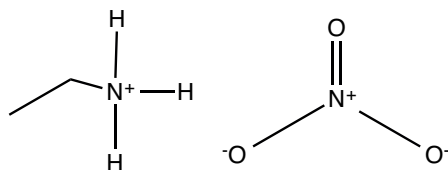


Figure 2.2: *Chemical structure of the ionic liquid ethylammonium nitrate.*

2.1.2 General properties and applications

The physical and chemical properties of ionic liquids depend on the molecular structure of the cation and the anion. Although the characteristic property of all types of ionic liquids is the melting point being below 100 °C, the exact melting temperature can vary based on the type of cation in terms of symmetry, capability of forming hydrogen bonds, and charge distribution, but also on the size of the anion [13]. Typi-

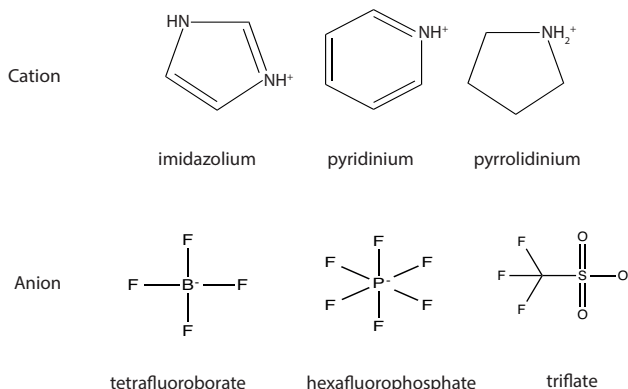


Figure 2.3: Chemical structure of typical cations and anions found in ionic liquids.

cally, ionic liquids made of a cation with low symmetry and incapable of forming hydrogen bonds have lower melting points. The importance of the anionic size is demonstrated by the comparison between the melting points of 1-Ethyl 3-methylimidazolium chloride (C_2C_1ImCl) and 1-Ethyl 3-methylimidazolium trifluoroacetate ($C_2C_1ImCF_3CO_2$) being $87\text{ }^\circ C$ [13, 15] and $-14\text{ }^\circ C$ [13, 16] respectively, the lower value being associated with the larger anion. Another fascinating property of ionic liquids is the very low vapor pressure, which is in most cases negligible. This makes them suitable materials for use in chemical processes of industrial relevance, such as separation by distillation. Moreover, ionic liquids show a high thermal stability, which in imidazolium based ionic liquids can extend up to $400\text{ }^\circ C$. For these ionic liquids the temperature window between the melting and the boiling point is thus larger than $400\text{ }^\circ C$. Further, these, ionic liquids show a high ionic conductivity (e.g. 88.2 mS/cm for the protic ionic liquid allyldimethylammonium TfO at $170\text{ }^\circ C$ [17, 18]), and wide windows of electrochemical stability (up to 6 V for aprotic ionic liquids) [18, 19], which become beneficial in for instance electrochemical applications.

Moreover, many polar and non-polar compounds can dissolve in ionic liquids [20]. Thus, ionic liquids have the potential to be used as solvents in traditionally multi-phase reactions to perform in single phase and overcome mass transfer limitations [21]. Other applications include dissolution of cellulose and metal deposition. More recently, it has been

discussed that the enzyme activity also benefits from the ionic liquid environment, which is very promising for the production of biofuels and for applications in biocatalysis [5]. Homogenous biocatalysts, have a higher partition coefficient in ionic liquids over the extract phase or the product, and can thus be immobilized in the ionic liquid phase [21]. Also, the product can be easily separated from the ionic liquid since the latter (acting as a solvent) is of low-volatility and can be recycled several times.

2.1.3 Synthesis

According to the distinction between protic and aprotic ionic liquids, two synthetic routes are commonly used. Aprotic ionic liquids are commonly synthesized by a metathesis reaction from a halide or similar salt of a desired cation (see Figure 2.4, right). Depending on the mis-

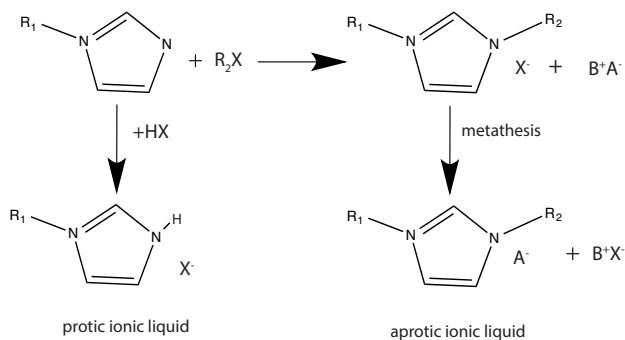


Figure 2.4: *Synthesis of protic and aprotic ionic liquids.*

cibility of the target ionic liquid with water there are two routes for metathesis. Water immiscible ionic liquids are prepared using a metal or ammonium salt, while water miscible ionic liquids are obtained from silver salt metathesis [22]. However, purification of water-miscible ionic liquids is more complicated due to the presence of by-products, is expensive, and exposes to the risk of silver contaminated products. Thus the most common synthetic route is by metathesis in aqueous solutions of a free acid or halide and its alkali metal or ammonium salt.

Protic ionic liquids are formed by proton transfer from a Brønsted acid to a Brønsted base at equimolar composition (see Figure 2.4, left). The purity of a protic ionic liquid depends on the purity of the starting reagents. According to Angell *et al.* if the $\Delta\text{p}K_a(=\text{p}K_a^{\text{base}}-\text{p}K_a^{\text{acid}})$ is higher than 10, the proton transfer is complete and the product is non-volatile and chemically stable [22, 23]. The major difference between aprotic and protic ionic liquids is the presence of exchangeable protons, typically but not exclusively on the cation.

2.2 Protic ionic liquids

If the proton transfer from the acid to the base is complete, the protic ionic liquid should solely consist of cations and anions. However, in practice this is not always the case and the presence of neutral species may result in a decreased ionic conductivity [24]. Lower conductivities may also arise from the formation of ion pairs, ion aggregation, or more complex ionic clusters [25]. In this context, the notion of "ionicity" (see also section 3.3) has been introduced to estimate the real contribution of the diffusing ions to the measured ionic conductivity [25]. The ionicity can be estimated either by employing the Walden plot¹ or by calculating the ratio of the molar conductivity obtained from impedance experiments (Λ_{imp}) to the molar conductivity calculated from NMR self-diffusion coefficients (Λ_{NMR}) using the Nernst-Einstein equation² [23, 24]. In a Walden plot, at a comparable viscosity ionic liquids with a higher ionicity also show a higher ionic conductivity. Angell *et al.* [23] have suggested a rationale to distinguish ionic liquids of different ionicity. This predicts that protic ionic liquids for which the $\Delta\text{p}K_a$ as measured in aqueous solutions is greater than 10 have a complete proton transfer and display an ideal Walden behavior [23]. The ionic conductivity is also dependent on the inter molecular interactions, and thus on the type of molecular structure of the ions. For instance, the conductivity of alkylammonium based protic ionic liquids is usually low (10 mS/cm) at 25 °C. Conductivity decreases by increasing the alkyl chain length in both imidazolium and ammonium based protic ionic liquids

¹A plot of the molar conductivity versus inverse viscosity in logarithmic scales.

² $\Lambda_{NMR} = \frac{F^2}{RT}(D_{cation} + D_{anion})$ where F is the Faraday constant and R is the universal gas constant, T is temperature, D_{cation} is the self-diffusion coefficient of cation, and D_{anion} is the self-diffusion coefficient of the anion.

due to a restricted mobility of the ions as a result of the larger size of the cations or a more efficient packing. In heterocyclic protic ionic liquids conductivity increases for less symmetrical cations and lower molecular mass. For symmetrical heterocyclic cation with higher molecular weight the viscosity increases, which results in lower conductivity [26]. For applications in fuel cells, it is desirable that protic ionic liquids provide highly mobile protons and a Walden behavior as close as possible to ideal. The challenge is thus finding the most suitable structures of protic ionic liquids that can meet these requirements.

2.2.1 Application in fuel cells

One of the main applications of ionic liquids is in electrochemical devices, where ionic conductivity plays a key role. For the specific case of fuel cells, protic ionic liquids have attracted considerable attention for use in proton exchange membrane (PEM) fuel cells due to the presence of an exchangeable proton, as compared to aprotic ionic liquids that are most suitable for battery applications. Moreover, due to a high thermal stability and non-flammability, protic ionic liquids are at the spotlight for use in next-generation PEM fuel cells with a target operational temperature above 120 °C [14]. In addition, the possibility that protons can move through proton donor-acceptor sites can contribute to an increased conductivity and thus enhance the overall performance of the fuel cell [26].

The fuel cell is a clean electrochemical device in which chemical energy is transformed from the oxidation of hydrogen at the anode and the reduction of oxygen at the cathode into electricity, while water and heat are the only by-products [27] (more details in Appendix 1). This device is currently very relevant since the concern about environmental issues, air pollution and clean air legislations is encouraging research & development sectors in both academics and companies to find alternative and cleaner forms of power supply. Today fuel cells are commercially available and mainly used in large stationary power supplies, residential power stations, and portable devices. However, a large obstacle in the path of a broader commercialization is the high production cost, mainly related to the platinum catalyst and the electrolytic materials. As a result, many research programs are ongoing with the aim to improve the

functionality and reduce the overall cost of the current PEM fuel cell components.

One issue with the current PEM fuel cell technology is the operational temperature, which has to be below 100 °C to maintain the membrane's humidity. Evaporation of water at temperatures above 100 °C affects negatively the fuel cell's overall performance, as a consequence of the drastic decrease in proton conductivity [28]. On the other hand, higher operational temperatures are desired to provide, for instance, an enhanced tolerance of platinum to CO poisoning. To address these issues, anhydrous electrolytes with high conductivity at elevated temperatures, high thermal stability, and low volatility should be developed as alternatives to aqueous based electrolytes. By virtue of providing all these properties, protic ionic liquids are very interesting candidates for use in PEM fuel cells. Different research groups have reported several protic ionic liquids suitable for fuel cell applications. Yasuda *et al.* [14] have reported that diethylmethylammonium trifluoromethanesulfonate (DEMA-TfO) possesses excellent bulk properties and low overpotentials associated to catalytic reactions at the electrodes. They also showed that when prepared with an excess of the base this protic ionic liquid provides an enhanced proton conduction through the Grotthuss mechanism. In the same context, Nakamoto *et al.* [29] showed that the combination of bis(trifluoromethanesulphonyl)imide acid (HTFSI) and benzimidazole (BIm) at an equimolar ratio produces an electrochemically and thermally stable protic ionic liquid [29]. Noda *et al.* reported that Brønsted acid-base ionic liquids can be prepared by mixing different molar ratios of solid imidazole (Im) and solid bis(trifluoromethanesulphonyl)imide acid. The equimolar ratio of the mixture formed a protic ionic liquid that is thermally stable up to 379 °C [2, 30].

It is noteworthy that the properties of protic ionic liquids drastically change due to impurities such as water or at non-equimolar ratios of the Brønsted acid and base. Recent studies have also investigated the impact of adding a second compound on certain physicochemical properties [31, 32].

2.3 Binary mixtures

One way to tune the physicochemical properties of ionic liquids is by mixing with a second compound such as water, alcohols, or acetonitrile [18, 32]. These mixtures typically show a lower melting point, lower viscosity and higher conductivity than the pure ionic liquid [18]. This is a consequence of changed inter molecular interactions that include, but are not limited to, hydrogen bonds. The addition of a second compound can disrupt the native interactions (mainly electrostatic and hydrogen bonds) in the neat ionic liquid whereby new hydrogen bonds can form between the ionic liquid and the added compound. Depending on the nature and strength of these new bonds, new properties can be displayed by the binary system. As an example, the molar excess volume for the majority of the binary mixtures based on a protic ionic liquid and a polar solvent is negative in the entire composition range, which indicates that the hydrogen bonds formed between the ionic liquid and the solvent are stronger than the cation-anion bonds in the pure ionic liquid or the solvent-solvent bonds in the neat solvent [18]. As an example, density values as a function of composition for the ethylene glycol/ $C_2HImTfO$ binary mixture are shown in Figure 2.5.

While considering binary mixtures based on an ionic liquid and water, it has been observed that this mixing is exothermic for protic ionic liquids, due to an increased number of hydrogen bonds [18], and endothermic for aprotic ionic liquids. Also, results indicate that water interacts more strongly with protic than with aprotic ionic liquids [18]. The same behavior is also observed for the mixture of a protic ionic liquid and ethylene glycol [18, 33, 34]. The hydrophobicity/hydrophilicity of the anion also plays a role in the miscibility of an ionic liquid with water. For example, because the TFSI anion is more hydrophobic than BF_4 , the ionic liquid $C_4C_1ImTFSI$ is immiscible with water while $C_4C_1ImBF_4$ is miscible in the whole composition range [35].

Recently the interest in adding water to protic ionic liquids has increased due to the observation of interesting effects on the local coordination of cations and anions [36, 37]. In particular, for ammonium based protic ionic liquids it has been shown that water triggers the formation of nano-structured domains, an effect that depends on the relative water concentration [36]. Added water also affects other properties of

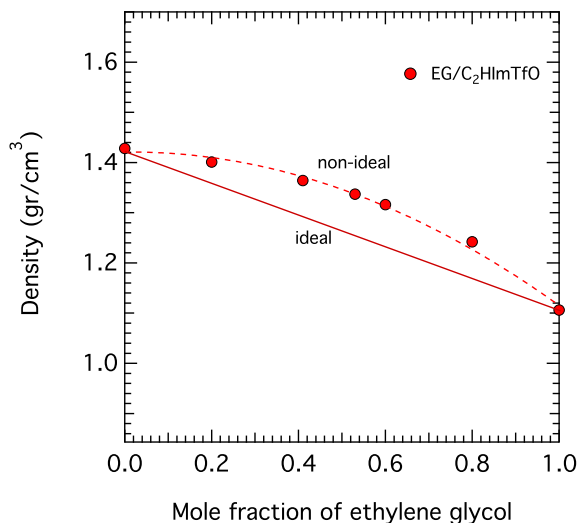


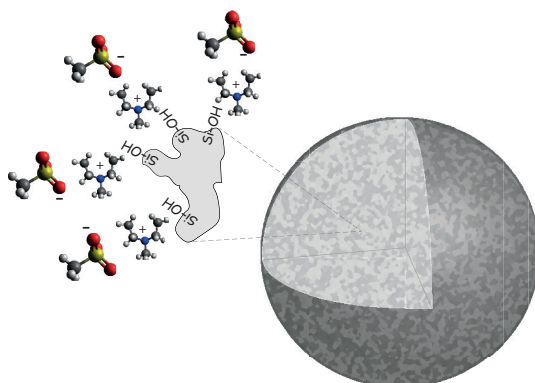
Figure 2.5: Density of the EG/C₂HImTfO binary system measured at 30 °C. The behavior expected by an ideal mixture is shown as a solid line.

ionic liquids, such as phase behavior, density, viscosity and conductivity [37–41]. Consequently, the addition of water can be employed to tune properties of relevance for applications in PEM fuel cells.

2.4 Effects of nano-confinement

Recently silica based materials have drawn attention as frameworks for retaining ionic liquids as alternative to polymer based membranes [42]. The incorporation of an ionic liquid into a porous solid results in a hybrid material also called 'ionogel' [43]. This can be achieved either by impregnation with an ionic liquid of nano-porous silica micro-particles [44], Figure 2.6, or through an in-situ sol-gel synthesis [43, 45]. While in the first type of ionogel the particles are held together by weak forces like hydrogen bonds or Van der Waals interactions, in the latter the whole network is covalently bound [43].

The immobilization of the ionic liquid into the nano-pores of the ionogel can affect both the phase behaviour and the transport properties.



Cartoon of a nano-porous silica micro-particle.

Figure 2.6: *Cartoon of a nano-porous silica micro-particle with nano-sized pores that can contain a protic ionic liquid.*

The effect is highly dependent on the pore size, the chemistry of the silica's pore walls and the molecular structure of the ionic liquid [46–49]. Studies have shown that the bulk properties of the ionic liquid can be retained in the central part of the pores while in the vicinity of the pore walls the interaction between silica and ionic liquid limits the mobility and changes the local conformation [50, 51]. Strategies are sought for limiting diffusion retardation while keeping the ionic liquid inside the nano-domains.

For applications in electrochemical devices, an ionic liquid should provide a fast and possibly selective ion motion. So, if an enhanced Li^+ -ion motion is required for Li-ion batteries, a selective H^+ -ion motion is desired in fuel cells. How fast ions, or more generally molecules, can move within a material depends on its transport properties, which include viscosity and mobility. Therefore, understanding the mechanism that underpins the mobility of the individual ions is crucial for the identification of a suitable ionic liquid and, possibly, a suitable binary system based on an ionic liquid and a neutral additive such as water or imidazole. With minor modifications, classical theories can reasonably describe the ionic conductivity and diffusivity in ionic liquids. These theories, as well as the basic mechanisms of proton transport, are explained in this chapter.

3.1 Self-diffusion

The random translational movement of molecules driven by thermal energy in an isotropic system is called Brownian motion. In such a system the molecules diffuse as a consequence of a concentration gradient and the diffusion is described by Fick's first law [52]:

$$J = -D \frac{dc}{dx} \quad (3.1)$$

where J is the molecule flux, D is the diffusion coefficient and dc/dx is the concentration gradient. Although the average displacement of molecules during time in the three dimensions is zero, the mean square displacement is not. The root mean square of distance Z_{rms} travelled by a molecule in one dimension is [53]:

$$Z_{rms} = \sqrt{2Dt} \quad (3.2)$$

Hence, D , also known as the self-diffusion coefficient, represents the rate of displacement of molecules over time and has the unit of m^2/s . In classical hydrodynamic systems the self-diffusion coefficient is related to the size of the molecular species (sphere) through the Stokes-Einstein equation:

$$D = \frac{k_b T}{f} \quad (3.3)$$

in which f is the frictional force, k_b is the Boltzman constant, T is the absolute temperature in K and f is in turn defined as:

$$f = c\pi\eta r_s \quad (3.4)$$

In equation 3.4, η is the viscosity of the solution, c is the shape factor, and r_s is the effective hydrodynamic (Stokes) radius of the diffusing molecular species. By combining equation 3.3 and 3.4 the Stokes-Einstein equation can be rewritten as:

$$D = \frac{k_b T}{c\pi\eta r_s} \quad (3.5)$$

Examples of self-diffusion coefficients measured for pure substances and for the ions of a typical ionic liquid are shown in Table 3.1.

When equation 3.5 is applied to the motion of large, rigid diffusing molecular species in the continuum of a solvent made up of small molecules, the c factor attains the value of 6. However, an empirical equation suggested by Chen *et al.* [53, 54] also shows that the c factor is reduced to 3.5 if the ratio of solvent/solute radii approaches 1.

$$c = \frac{6}{[1 + 0.695(r_{solvent}/r_{solute})^{2.234}]} \quad (3.6)$$

Table 3.1:

Examples of self-diffusion coefficients measured for pure substances and for the ions of an ionic liquid (C₂HImTFSI) at 30 °C.

	Water [57]	Cyclohexane [57]	C ₂ HIm (cation) [58]	TFSI (anion) [58]
D (m ² /s)	2.61×10 ⁻⁹	1.65×10 ⁻⁹	2.95×10 ⁻¹¹	2.27×10 ⁻¹¹

In the case of ionic liquids equation 3.5 should be applied carefully since the ions are both solute and solvent, differently from the case of conventional electrolytes. In this context, Tokuda *et al.* have shown that in ionic liquids the Stokes-Einstein equation can describe the diffusive behavior only when the c factor is reduced to ca. 4 [24]. Further, the value of c also seems to vary slightly between ionic liquids, and to be different for cations and anions [55, 56].

3.2 Conductivity

While the Stokes-Einstein equation describes the diffusion of molecules regardless their charged or non-charged state, conductivity specifically refers to the motion of charged molecules. How easily charged molecules, or ions, can move within a media is an intrinsic property that reflects the media's resistance to the flow of charges. The molar conductivity, Λ_m , that takes into account the number of ions present in the electrolyte is defined as:

$$\Lambda_m = \frac{\kappa}{C} \quad (3.7)$$

where κ is the conductivity in siemens per meter (S/m), C is the molar concentration of the electrolyte (mole/L), and Λ_m has the unit of Sm²/mol. In strong electrolytes such as strong acids and ionic solids the dissociation of ions is complete and the molar conductivity decreases only slightly with concentration due to the fact that the ions interact weakly with each other. By comparison, in weak electrolytes the molar conductivity decreases more drastically with concentration as a result of significant interactions between the ions, Figure 3.1. At the limit of infinite dilution the ions are considered as well-separated and non-

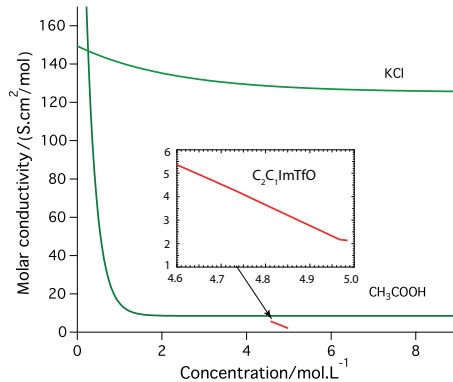


Figure 3.1: Dependence of the molar conductivity on the electrolyte concentration in strong (e.g. KCl) and weak (e.g. CH₃COOH) electrolytes (reproduced from ref. [52]), as well as in the C₂C₁ImTfO ionic liquid [58].

interacting, and the limiting molar conductivity, Λ_m^o , is expressed as:

$$\Lambda_m^o = \nu_+ \lambda_+^o + \nu_- \lambda_-^o \quad (3.8)$$

where ν_+ and ν_- are the number of cations and anions per formula unit of the electrolyte (for example $\nu_+ = \nu_- = 1$ in HCl, and $\nu_+ = 2$, $\nu_- = 1$ in Na₂SO₄), and λ_+^o and λ_-^o are the molar conductivities at infinite dilution of cations and anions, respectively [52].

As Friederich Kohlrausch showed, in strong electrolytes the molar conductivity is linearly dependent on the square root of concentration at low concentrations:

$$\Lambda_m = \Lambda_m^o - K\sqrt{C} \quad (3.9)$$

while in weak electrolytes the molar conductivity depends on the degree of ionization α :

$$\Lambda_m = \alpha \Lambda_m^o \quad (3.10)$$

or, implementing the pK_a^1 of the solution a new relation, known as Ostwald's dilution law is obtained:

$$\frac{1}{\Lambda_m} = \frac{1}{\Lambda_m^o} + \frac{\Lambda_m C}{\text{pK}_a (\Lambda_m^o)^2} \quad (3.11)$$

¹ $\text{pK}_a = -\log K_a$, where pK_a is the logarithmic acid dissociation constant (K_a)

The dependence of conductivity on temperature for most solids and crystalline materials follows an Arrhenius behavior (eq. 3.12):

$$\sigma = \sigma_0 \cdot e^{\frac{-E_a}{RT}} \quad (3.12)$$

where σ is the conductivity, E_a is the activation energy, T is the temperature, and R is the gas constant. In liquid electrolytes the VFT (Vogel-Fulcher-Tamman) equation better describes the dependence of conductivity (but also fluidity) on temperature:

$$\sigma = \sigma_0 \cdot e^{\frac{-D_f \cdot T_0}{T - T_0}} \quad (3.13)$$

where σ is the conductivity, T_0 is a temperature related to the glass transition temperature (T_g) and D_f is a parameter inversely proportional to the fragility of the liquid [11, 59]. The VFT equation becomes useful when conductivity (or fluidity) is measured for a very wide temperature range extending down to the glass transition temperature. This equation allows to distinguish between more or less fragile materials [11]. The fragility of a material can be estimated from the value of the fragility parameter, D_f , which for the ionic liquid $\text{PYR}_{24}\text{TFSI}$ and $\text{PYR}_{14}\text{TFSI}$ is 6.37 and 5.78 [59], respectively. These values are comparable with that of toluene ($D_f=5.6$) [60], which is known to be a very fragile glass-forming liquid .

3.3 Ionicity

The degree of ionic dissociation is a concept easily applicable to conventional electrolytes (acid or alkaline aqueous solutions), in which the ions are solvated by water molecules. By contrast, in anhydrous electrolytes like ionic liquids the ions are not solvated and act as solvent and charge carriers simultaneously. For such molecules the degree of ionic dissociation can be evaluated by either the 'ionicity' approach or by means of a 'Walden plot' [61].

The concept of ionicity was introduced by Watanabe *et al.* [25], and was defined as a dimensionless value, $\Lambda_{imp}/\Lambda_{NMR}$, where Λ_{imp} is the molar conductivity obtained from impedance measurements and Λ_{NMR}

is the molar conductivity obtained from the self-diffusion coefficient through the Nernst-Einstein equation. This ratio indicates how well the diffusing ions really contribute to the transport of charge. The expression of ionicity can be understood from the following relations. The ionic mobility, u , and the molar conductivity, λ , are related as:

$$\lambda = zuF \quad (3.14)$$

where F is the Faraday constant ($F=N_A \cdot e$) and z is the charge of the diffusing species [52]. According to the Einstein relation also the diffusion coefficient depends on the ionic mobility, (u), through:

$$D = \frac{uRT}{zF} \quad (3.15)$$

Thus, by combining equation 3.14 and 3.15 we obtain:

$$\lambda = zuF = \frac{z^2DF^2}{RT} \quad (3.16)$$

and for a mixture of positively and negatively charged ions (recall equation 3.8):

$$\Lambda_m^0 = \frac{(\nu_+z_+^2D^+ + \nu_-z_-^2D^-)F^2}{RT} \quad (3.17)$$

In the case of ionic liquids, where $z_+=z_-=1$ and $\nu_+=\nu_-=1$, this expression simplifies to:

$$\Lambda_m^0 = \frac{(D^+ + D^-)F^2}{RT} \quad (3.18)$$

This relation gives an estimation of the molar conductivity expected if all species diffuse in a dissociated state. In ionic liquids, however, this is not always the case, and the $\Lambda_{imp}/\Lambda_{NMR}$ ratio therefore attains values lower than unity, typically in the range 0.5–0.7.

In the second approach, an empirical observation known as the Walden's rule shows that the product $\Lambda_m\eta$ is a constant, which implies that $\Lambda_m \propto 1/\eta$ or more directly that $\Lambda_m \propto D$. Yoshizawa *et al.* proposed the use of the Walden plot to compare the ionicity of different ionic liquids [23], a qualitative scale where molar conductivity is plotted versus

inverse viscosity in logarithmic scales, Figure 3.2. In this plot, poor, good, and superionic ionic liquids can be distinguished, based on their deviation from the ideal behavior (*i.e.* that of a 1M aqueous solution of KCl). Those ionic liquids that are closer to the ideal line are also better dissociated. In Figure 3.2, several ionic liquids are compared, showing a large span of different behaviors.

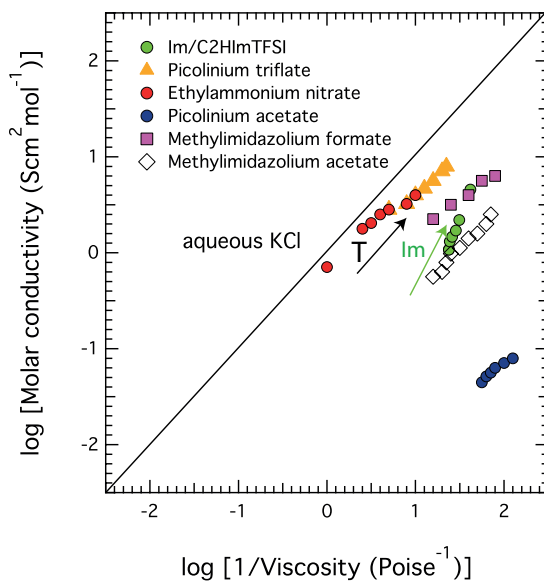


Figure 3.2: Walden plot for to the binary system of imidazole and $\text{C}_2\text{HImTFSI}$ (green) and for ionic liquids reported in ref.23: Picolinium triflate (yellow), Ethylammonium triflate (red), Picolinium acetate (blue), Methylimidazolium formate (pink), and Methylimidazolium acetate (white). The arrows show the increase of temperature (black) and imidazole concentration (green).

3.4 Proton transfer mechanism

There are two mechanisms of proton transfer, the *vehicular* and the *Grotthuss* type. In the vehicular type the proton is carried by the ionic species through the medium, Figure 3.3 A, while in the Grotthuss mechanism the proton transfers by hopping from a proton 'excess' site to a proton 'deficient' site mediated by hydrogen bonds in the liquid, Figure 3.3 B. Therefore, the existence of an extended hydrogen bonded network is a prerequisite for the occurrence of the Grotthuss type of proton

transfer [62]. On the other hand, proton transfer requires frequently breaking-forming bonds which is only possible in a weakly hydrogen bonded network [63]. The Grotthuss (or "structural diffusion") mechanism in water can be described by frequently breaking and forming hydrogen bonds when the proton defect site is at the centre of symmetry of the hydrogen bonded network. Hydrogen bonds in proton excess regions are contracted and the hydrogen bond breaking-forming process occurs in the outer shell of the complex [63]. In this way, proton diffuses through a propagating hydrogen-bond re-arrangement, Figure 3.3 B.

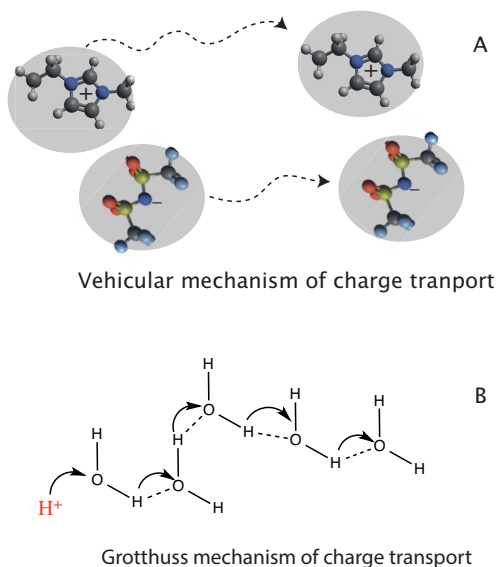


Figure 3.3: Vehicular mechanism of proton transfer in $C_2C_1ImTFSI$ (A) and Grotthuss mechanism of proton transfer in water (B).

In aprotic ionic liquids the charge transfer occurs mainly through the vehicular mechanism and is therefore dependent on the diffusion rate of the molecular ions. The universal behavior that emerges when conductivities are compared on T_g -scaled Arrhenius plots indicates that viscosity is the main factor determining ionic conductivity. This has, for instance, been verified for LiTFSI doped ionic liquid such as pyrrolidinium bis(trifluoromethanesulfonyl)imide (PyrTFSI) [59].

By contrast, in protic ionic liquids, the proton of the cation may transfer through both the vehicular and the Grotthuss mechanism. Although the cation carries the positive charge through the medium by diffusion, the presence of proton donor and acceptor sites in protic ionic liquids enables the formation of extended hydrogen bonds, which could facilitate the proton hopping mechanism as it occurs in other hydrogen bonded liquids like water. Although theoretically possible, the proton transfer through the Grotthuss mechanism in protic ionic liquids is currently debated [64–66]. One method to assess the occurrence of the Grotthuss mechanism is to verify that the D_{NH}/D_{cation} ratio is higher than unity, where D_{NH} is the diffusion coefficient of the protic proton, Figure 3.4. However, Blanchard *et al.* have discussed the risk of overestimating the self-diffusion values as a result of fast proton exchanges between water (impurities) and protic sites in the time-frame of the diffusion experiments [64]. Clearly, the verification of the Grotthuss mechanism in protic ionic liquids is not straightforward.

Recent studies have shown that in non-stoichiometric mixtures of a Brönsted acid and a Brönsted base the proton transfer through structural diffusion (Grotthuss mechanism) is promoted and assisted by an hydrogen bonded network of intermediate strength [30, 66, 67]. Kreuer *et al.* have examined the effect of adding imidazole to phosphoric acid at a 1:2 molar ratio, but found that the proton conductivity decreases due to the removal of protons from the hydrogen bonded network in H_3PO_4 and the consequent formation of too stable hydrogen bonded ion pairs [67].

3.5 Intermolecular forces

While in common salts like NaCl the ionic bond is the dominant force between the cation and the anion, in ionic liquids the situation is more complex due to a competition between Coulombic attraction, hydrogen bonding and dispersion forces [68–70]. This is also believed to be the origin of the unique properties displayed by this class of materials. For instance, it has been argued that the presence of local and directional hydrogen bonds in aprotic ionic liquids increases fluidity. Hydrogen bonds can also lower the melting point, and decrease the viscosity and the enthalpy of vaporization of ionic liquids [71, 72].

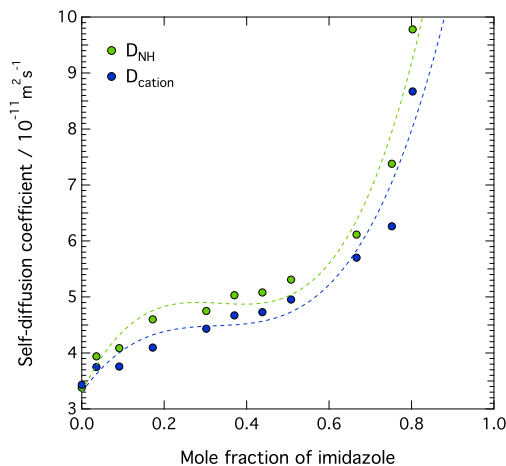


Figure 3.4: Self-diffusion coefficients measured at 30 °C for the imidazolium cation (D_{cation} , blue) and the proton bound to the nitrogen atom (D_{NH} , green) as a function of composition in the binary mixture of $\text{C}_2\text{HImTFSI}$ and imidazole (**PaperV**).

The contribution of dispersion forces to the overall interaction energy in aprotic ionic liquids has been evidenced by density functional theory (DFT) calculations [73]. However, in a 'Coulombic dominant fluid' it is very hard to distinguish between hydrogen bonds and dispersion forces. Nevertheless, Ludwig *et al.* have recently shown that hydrogen bonds and dispersion forces each share 10 percent of the overall interaction energy, which is about 50 kJ mol⁻¹ [69]. In turn, dispersion forces can be considered to have contribution *within* a cation-anion pair (strengthening the hydrogen bond between the cation and the anion) and *between* ion-pairs [69]. Local and directional hydrogen bonds can be studied by far-infrared spectroscopy which provides experimental evidence to distinguish these forces in protic ionic liquids [69, 70]. For example, Fumino *et al.* combined DFT calculations and far-infrared spectroscopy to quantitatively distinguish between hydrogen bonds and dispersion forces in the protic ionic liquid trihexylammonium triflate [70].

To conclude, understanding the balance between hydrogen bonds, electrostatic attraction and dispersion forces in protic ionic liquids is key to elucidate the structure-property relationship. Several studies also suggest that this balance can be affected when an ionic liquid is mixed with

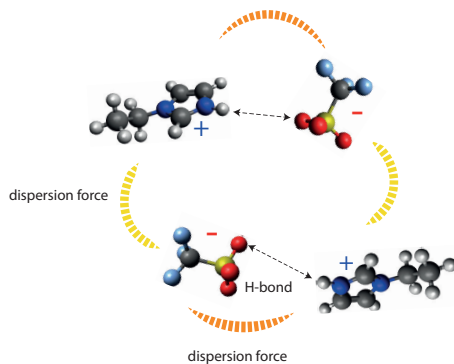


Figure 3.5: Schematic picture of intermolecular interactions in ionic liquids that include Coulombic attraction, dispersion forces and hydrogen bonds, reproduced from ref.69

an organic solvent or water, which further results in changed physical and chemical properties [38–41]. More precisely, understanding how added compounds can affect the specific nature of cation-anion interactions will be crucial to design new ionic liquid structures with desired properties, *e.g.* a selective proton transport.

Characterization techniques

In this thesis different experimental techniques have been used to investigate several physicochemical properties. To evaluate the transport properties we have employed nuclear magnetic resonance (NMR) diffusometry and impedance spectroscopy, while for the analysis of intermolecular interactions ^1H NMR spectroscopy and vibrational spectroscopy (including Raman and infrared) were used. It is notable that these techniques are non-destructive. The phase behavior of pure or mixed liquids was studied by differential scanning calorimetry (DSC) and the thermal stability by thermal gravimetry analysis (TGA). Both the basic principles of these techniques and the experimental details related to the measurements are described in this chapter.

4.1 NMR spectroscopy

NMR spectroscopy is an analytical method based on the magnetic properties of the atomic nuclei typically used to study the structure of molecules and investigate the chemical environment of the atoms. The nucleus of interest, mainly the proton in this thesis, absorbs the electromagnetic radiation at a certain characteristic frequency. Thus, in an NMR spectrum absorption intensities are plotted as a function of the chemical shift, a parameter that is defined as:

$$\delta(ppm) = 10^6 \times \frac{\nu - \nu_{ref}}{\nu_{ref}} \quad (4.1)$$

where ν is the resonance frequency of the sample and ν_{ref} is the resonance frequency of a reference such as tetramethylsilane (TMS). To obtain the chemical shift of the protons present in ionic liquids, ^1H NMR spectra were collected on a 400 MHz Varian NMR spectrometer over 8 scans with 1 second of recycling delay. The spectra were referenced to a standard octamethylcyclotetrasiloxane.

4.2 Diffusion NMR

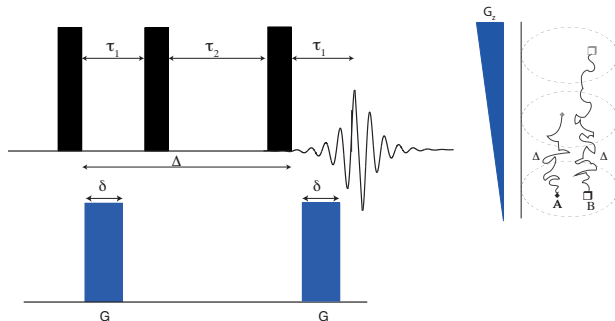


Figure 4.1: (Left) the pulse sequence for the measurement of self-diffusion based on the PFG-stimulated echo. In this sequence τ_1 is the first time interval, τ_2 is the second time interval, Δ is the diffusion time, δ is the length of the gradient pulse, and G is the gradient strength. (Right) schematic illustration of the local field experienced by diffusing molecules during the first gradient pulse that does not match with the local field experienced by them during the second gradient pulse due to diffusion time (Δ), reproduced from ref. 53.

Pulsed field gradient stimulated-echo (PFG-STE) NMR spectroscopy is a non-destructive technique that is suitable for the characterization of diffusive processes. [74]. Figure 4.1 (left) shows the pulse sequence used in this thesis for diffusion measurements. The first 90° pulse turns the magnetization to the transverse plane. After a time interval τ_1 , a second 90° pulse rotates the magnetization to the negative z direction. After a time interval τ_2 , a third 90° pulse returns the magnetization to the transverse plane where the signal is acquired after time τ_1 . The

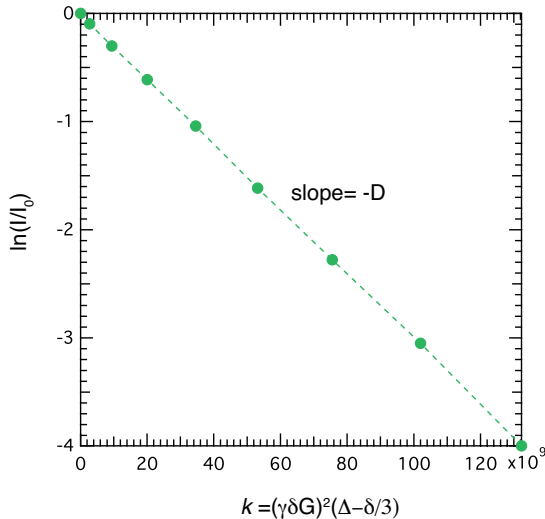


Figure 4.2: The normalised magnetic intensity versus k for the cation in $C_2HImTFSI$ /water system. The slope gives the self-diffusion, D , of the diffusing entity.

gradient pulse imposes a spatially dependent phase on the diffusing species during the diffusion time Δ . The magnetization will be refocused after the second gradient pulse. The complete recovery of the signal depends on if the spins remain in the same place when the two gradient pulses are applied. If spins move, then the local field experienced by them is not similar to the initial position, therefore the signal will be attenuated. Hence, the attenuation depends on how fast the diffusive species are displaced from their initial position, Figure 4.1 (right).

The decay of the magnetization intensity occurs due to transversal relaxation (T_2), longitudinal relaxation (T_1), and diffusion (D) of the molecule. The specific benefit in PFG stimulated-echo pulse sequence is that the loss of magnetization intensity occurs mainly by longitudinal relaxation, T_1 , which is slower compared to the T_2 relaxation. Transverse magnetization loss occurs in shorter time period τ_1 , therefore less sensitive to the transverse relaxation rates (T_2) of the molecules. The relation between the decay of the magnetization and the self-diffusion coefficient of a diffusing molecule is defined by the Stejskal-Tanner [53]

expression as follows:

$$I = I_0 \cdot \exp^{-k} = I_0 \cdot \exp - (\gamma \delta G)^2 D (\Delta - \delta/3) \quad (4.2)$$

where I is the signal intensity, I_0 is the signal intensity of spin-echo at zero gradient including T_1 and T_2 terms, G is the gradient strength, D is the self-diffusion coefficient, γ is the gyromagnetic ratio, δ the length of the gradient pulse, and Δ is the diffusion time [53]. As Figure 4.2 shows D can be extracted from the slope of the normalized intensity (natural logarithmic scale) versus k .

In this thesis pulsed field gradient nuclear magnetic resonance (PFG NMR) experiments were performed on a Bruker Avance 600 spectrometer. The applied linear gradient was varied in the range 0–1200 G cm^{-1} , while the diffusion time Δ and the pulse duration δ were set to 150 and 0.6–3 ms respectively. The number of acquisitions in each experiment was 8 and the relaxation delay was 10–15 s according to the specific T_1 values measured for the different liquids and concentrations. To ensure that thermal convection did not affect our results, we run the diffusion NMR experiments for different Δ values (*e.g.* 100, 150, and 200 ms) whereby the self-diffusion coefficients were observed not to depend on D at 30 °C.

4.3 Ionic conductivity

The ionic conductivity of an electrolyte (having the unit of siemens per meter, S/m) can be obtained by measuring its resistance to an applied potential difference. Typically, the electrolyte is kept between two electrodes with defined geometry and fixed distance, while an alternating potential is applied. The conductance G is expressed in siemens (S) and is the inverse of the resistance R (Ω). Ionic conductivity is then expressed as:

$$\kappa = \frac{l}{A} \cdot \frac{1}{R} \quad (4.3)$$

where κ is the conductivity, A is the area of the electrodes, l is the distance between electrodes, R is the resistance, and $G=1/R$ is the conductance.

In this work, conductivity measurements were performed on a Meterlab model CDM 210 conductivity meter instrument that is suitable only for liquid samples and for temperatures below 90 °C. The samples were equilibrated for 30 minutes at 30 °C before collecting data. A dosimeter was used to carefully control the amount of water added to the ionic liquid. The instrument was calibrated with a 0.01 M aqueous solution of KCl, which serves as an ideal electrolyte.

4.4 Density and viscosity measurements

In this thesis the density of the mixtures were measured by an Anton Paar density meter at 30 °C. The viscosity was also measured by an Anton Paar rheometer model MCR 300 with cone and plate geometry of $\phi=50$ mm, angle=1°, and gap 52 μm at 30 °C. The shear frequency were adjusted to 10 Hz for the investigated binary systems.

4.5 Vibrational spectroscopy

By vibrational spectroscopy, that here includes both infrared and Raman spectroscopy, the vibration of molecules can be probed. Although chemical bonds in compounds are usually considered as well defined in bond lengths and bond angles, atoms can in fact displace from these average values in an oscillatory manner. In the classical approach, molecules are described as atoms held together by a spring, see Figure 4.3. The force constant (k), represents the bond energy and m is the mass of the atom. The frequency of vibration is related to both k and m through [75]:

$$\nu = \frac{1}{2\pi} \sqrt{k \left(\frac{1}{m_1} + \frac{1}{m_2} \right)} \quad (4.4)$$

Depending on the type of displacement of the atoms relative to each other, molecular vibrations can be classified as stretching, bending, wagging *etc.*, as shown in Figure 4.4.

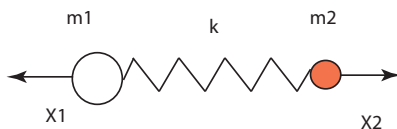


Figure 4.3: Classical model of the simple case of a diatomic molecule where two atoms of mass m_1 and m_2 are held together by a spring force k .

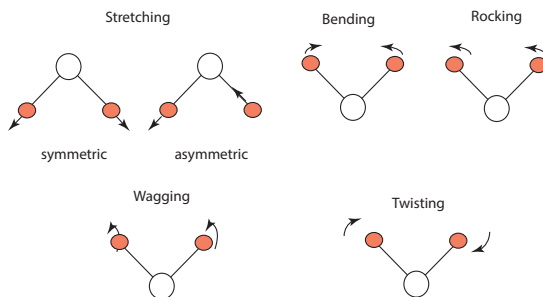


Figure 4.4: Examples of vibrational modes in a diatomic molecule.

Quantum mechanical argumentations predict that the energies of vibration are discrete and defined by the following equation [75]:

$$E = (n + 1/2)\hbar\sqrt{k/\mu} \quad (4.5)$$

where $n = 0, 1, 2, \dots$ is the vibrational quantum number, \hbar is Planck constant, k is the spring constant and μ is the reduced mass defined as $(m_1 + m_2)/m_1 \cdot m_2$. The energy levels $E_{0,1,2,\dots}$ are equally distanced, with E_0 ($n=0$) being the ground state or ground energy level, and E_1 ($n=1$) representing the first excited level, etc. According to selection rules transitions are allowed only between adjacent levels, *i.e.* $\Delta n = \pm 1$, and occur when the energy difference between these levels equals the energy of the incoming light $\hbar\omega$, where ω is the light's frequency. While in infrared spectroscopy a vibration is excited by absorption of light, in Raman spectroscopy energy transitions occur by means of an inelastic scattering process. Further details on these two distinct techniques are provided below.

4.5.1 Infrared spectroscopy

In infrared spectroscopy a molecular vibration is excited when the energy of the incoming light matches that of an energy of transition, *e.g.* from E_0 to E_1 . A molecular vibration is infrared active if the dipole moment (μ) changes during the vibration. The measured infrared intensity is:

$$I_{IR} \propto \text{concentration} \times \Delta\mu \quad (4.6)$$

The measured infrared band intensity is proportional to the square of the change in dipole moment and the condition for a vibration to be infrared active is

$$\left(\frac{\partial\mu}{\partial Q} \right) \neq 0 \quad (4.7)$$

where Q is the vibrational amplitude [75].

4.5.2 Attenuated total reflectance (ATR)

Infrared spectra measured in the attenuated total reflectance (ATR) mode, are obtained using a crystal with high refractive index and excellent infrared transmission. The sample should be in perfect contact with the crystal, wherefore the technique is best suited for liquids and soft materials like polymers. In ATR the angle of incident light is greater than the critical angle and therefore total internal reflectance can occur. As Figure 4.5 shows, the incident light penetrates into the sample at the reflectance point as an "evanescent wave". If the frequency of the incident light is within the range of the frequencies that are absorbed by material, the reflection will be attenuated while if that is far from the absorbance region the light will be totally reflected [75].

The critical angle follows the relation below:

$$\theta_C = \sin^{-1} \left(\frac{\eta_2}{\eta_1} \right) \quad (4.8)$$

where η_2 is the complex refractive index of the sample and η_1 is the complex refractive index of the crystal. The complex refractive index of the sample consists of a real part and an imaginary part:

$$\eta = n + ik \quad (4.9)$$

The real part relates to regular refractive index when there is no absorption and the imaginary part relates to the situation when absorption occurs. Moreover, k is directly related to the extinction coefficient in the Lambert-Beer law and the total absorption intensity is related to the penetration depth of the "evanescent wave" into the sample. Normally the penetration depth (d_p) is a function of the incident light wavelength, the refractive index of the crystal (n_p) and the ratio of the refractive indices of the sample and crystal ($n_{sp}=n_2/n_1$) as below:

$$d_p = \frac{\lambda}{2\pi n_p (\sin^2\theta - n_{sp}^2)^{1/2}} \quad (4.10)$$

The penetration depth (d_p) in the ATR method is usually in the order of 2-15 μm [75].

In this work infrared spectra were collected with a Perkin Elmer spectrometer using the attenuated total reflection (ATR) mode and pouring the solutions over a single-point reflectance diamond crystal. For each

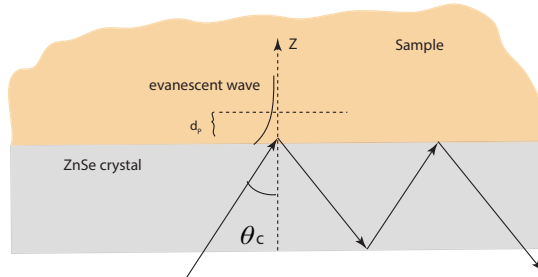


Figure 4.5: Basic principles of Attenuated Total Reflectance (ATR), reproduced from ref. [75].

sample 32 scans were averaged with a nominal spectral resolution of 2 cm^{-1} . The full spectral range $400\text{--}4000\text{ cm}^{-1}$ was investigated.

4.5.3 Raman scattering

Raman spectroscopy is based on a light scattering phenomenon. As a result of the interaction with the incident light, molecular vibrations are excited to a virtual state before relaxing back to a lower energy level. Because of the law of energy conservation, if the final level is of higher energy than the initial one, scattered light is of lower energy (and longer wavelength) than the incoming light (red arrow, Stokes). If the final level is of lower energy than the initial level, scattered light is of higher energy (and shorter wavelength) than the incoming light (blue arrow, anti-Stokes). These cases are presented in Figure 4.6.

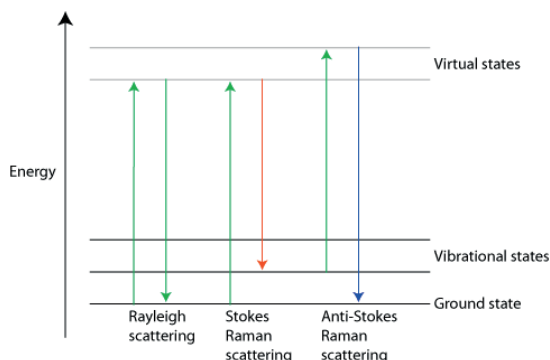


Figure 4.6: *Rayleigh, Stokes and anti-Stokes scattering.*

Most of the scattered light has the same energy as the incoming, and the elastic process is called Rayleigh scattering. Only a minor part of the light is scattered at a different energy, which is lower in the Stokes scattering and higher in the anti-Stokes, see figure 4.6. Since at normal conditions most of the molecules are found in the ground level of energy, Stokes events are more probable than anti-Stokes. Moreover, Rayleigh scattering that involves no exchange of energy occurs ca. 10^6 times more than the inelastic events, and must be eliminated for Raman spectra to be obtained. The intensity of Raman scattering radiation is defined by the following relation:

$$I_R \propto \nu^4 I_0 N \left(\frac{\partial \alpha}{\partial Q} \right)^2 \quad (4.11)$$

where I_0 is the incident laser intensity, N is the number of scattering molecules in a given state, ν is the frequency of the exciting laser, α is the polarizability of the molecules, and Q is the vibrational amplitude. The polarizability of the molecule, α , determines whether a molecular vibration is Raman active or not, according to: [75]

$$\left(\frac{\partial \alpha}{\partial Q} \right) \neq 0 \quad (4.12)$$

An example of Raman and infrared spectra is presented in Figure 4.7, which shows that the C-H, N-H and O-H stretching modes in pure $C_2HImTFSI$ are more intense in infrared than in Raman spectroscopy.

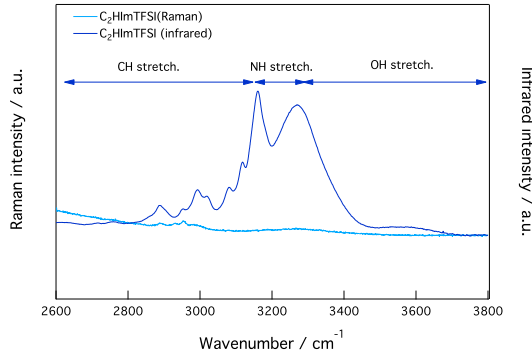


Figure 4.7: *High frequency region of Raman and infrared spectra for pure $C_2HImTFSI$.*

4.5.4 The Raman spectrometer

Raman spectra were recorded with an InVia Reflex Renishaw spectrometer, equipped with three lasers (532, 630, and 785 nm). The 785 nm line of a diode laser and the 532 nm line of an Ar-ion laser were used as the excitation source to collect Raman spectra of the imidazolium and

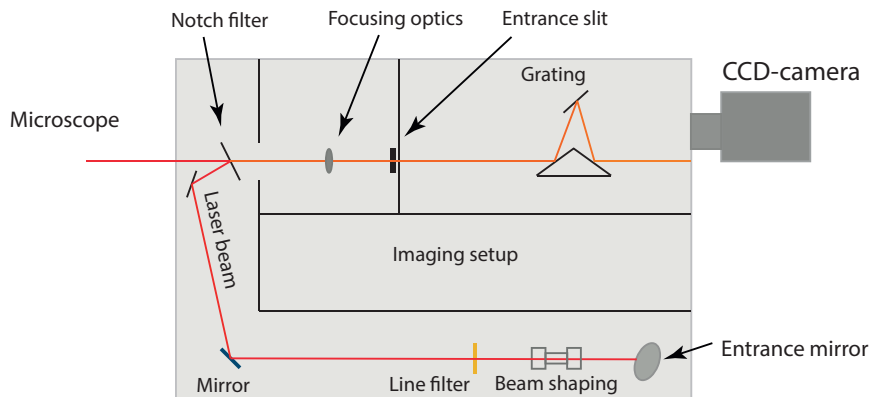


Figure 4.8: Setup of the Raman spectrometer used in this thesis.

ammonium based ionic liquids investigated in this thesis, respectively. The Raman spectrometer is also equipped with three different gratings (with 1200, 1800, and 2400 lines/mm) and a holographic notch filter. For high resolution measurements the 1800 grating was used. The notch filter is used as a mirror to direct the laser into the microscope and as a filter to remove the Rayleigh scattered light. The inelastically scattered light is detected with a two dimensional charge coupled device (CCD) camera, see Figure 4.8. In this work the 785 nm line was coupled with a 1200 l/mm grating and the 532 nm line with a 2400 l/mm grating. Under these conditions the spectral resolution is always better than 2 cm^{-1} . Recorded spectra were typically accumulated during 4-10 scans with a duration of 10 seconds each.

4.6 Differential scanning calorimetry

Differential scanning calorimetry (DSC) is a thermo-analytical technique by which the difference in heat flow between the sample and a reference is measured as a function of temperature. DSC is suitable to study thermal phenomena such as phase transitions, *e.g* melting and crystallization, glass transition, and heat capacity changes in a material. There are two basic types of DSC, the heat flux DSC and the power compensation DSC.

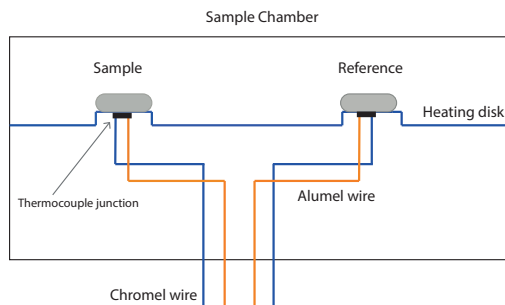


Figure 4.9: The schematic picture of the sample chamber in DSC setup where the heat flux is measured.

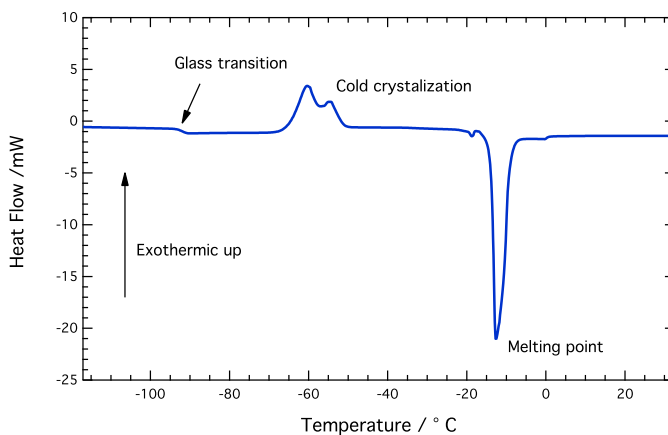


Figure 4.10: A DSC trace recorded during heating for the $C_2C_1ImTFSI/water$ mixture at a molar concentration equal to 1:1.

In this thesis a heat flux DSC was used, using a disk-type measuring system, where heat exchange occurs through a disk that serves as a support for the sample and the sample reference (see Figure 4.9). Two isolated pans, one containing the sample and one empty (the reference) are symmetrically positioned at the centre of the disk through which heat passes. Both disks are equipped with thermocouples that measure the temperatures of the sample and of the reference accurately. The rate of temperature increase is accurately controlled by a software. The

rate of temperature $\Delta T/\Delta t$ is equal for both sample and reference. However, the heat flow is different for sample and reference due to phase transitions in the investigated material. The rate of heat flow is plotted versus temperature change. This allows to measure all thermal transitions in materials such as glass transition, crystallization, melting where heat flow rate changes the released or absorbed heat during the transition. Depending on the nature of transition the heat flow could be exothermic (as in crystallization) and endothermic (as in melting). A typical DSC trace that shows both a glass transition, a crystallization and a melting is given in Figure 4.10.

4.7 Thermogravimetric analysis (TGA)

Thermogravimetric analysis (TGA) is also widely used to characterize the thermal properties of materials. In TGA the material is subjected to a constant heating rate, whereby the weight loss as a function of temperature is monitored. Weight changes occur during phase transitions such as vaporisation, chemical phenomena such as desorption, dehydration, and structural condensation and finally decomposition. Hence, the stability of a material within the investigated temperature range can be precisely determined.

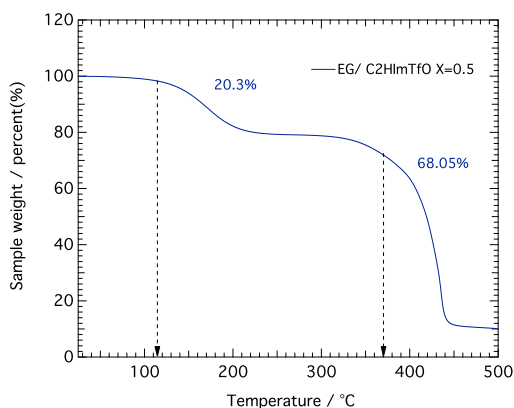


Figure 4.11: Thermogravimetric analysis of the EG/C₂HIMTfO mixture with a mole fraction of EG equal to $x=0.5$.

In this work TGA is used to study the thermal stability of ionic liquid based systems, including hydrated ionic liquids and the binary system of C₂HImTfO and ethylene glycol. Figure 4.11 shows the TGA plot of a C₂HImTfO/ethylene glycol mixture, in which the first step relates to the loss of ethylene glycol (at 114 °C) and the second step to the decomposition of C₂HImTfO (at 379 °C).

Results and discussions

In this chapter, the results obtained during the course of my PhD program are retrospectively discussed. In particular, the effect of adding water to the transport properties (**Paper I** and **Paper III**) and to the local coordination (**Paper II** and **Paper III**), the importance of hydrogen bonds to achieve high ionicity and thermal stability (**Paper III** and **Paper V**), as well as the effect of confining ionic liquids into nano-sized domains (**Paper IV** and **Paper VI**) are analysed in a broader scientific context. Finally the behavior of ionic liquids upon the addition of different neutral molecules (i.e. water, imidazole, and ethylene glycol) is also compared. The molecular structure of the ionic liquids considered in this thesis, *i.e.* $C_2C_1\text{ImTFSI}$ and $C_2C_1\text{ImTfO}$ (aprotic), and $C_2\text{HImTFSI}$, $C_2\text{HImTfO}$ and DEMA-OMs (protic), as well as the structure of the neutral molecules water, imidazole, and ethylene glycol are shown in Figure 5.1.

5.1 Self-diffusion in ionic liquids

Figure 5.2 shows the self-diffusion coefficients of the pure ionic liquids investigated in this thesis, except DEMA-OMs that is in the solid state at room temperature. In all investigated ionic liquids the cation diffuses faster than the anion. This difference had been predicted by molecular dynamics simulations [76] and has also been experimentally

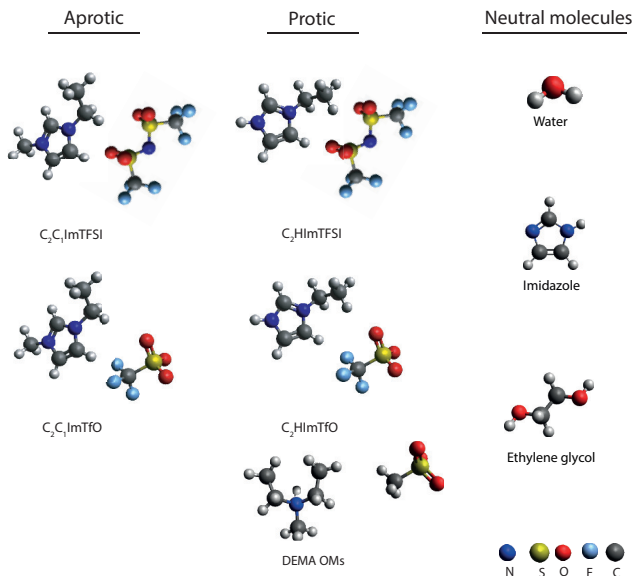


Figure 5.1: Chemical structure of the ionic liquids and the neutral compounds considered in this thesis.

observed by other authors [77, 78]. This is believed to be a result of the larger activation energy for diffusion associated to anions as compared to cations, as discussed for the ionic liquids $C_1C_1\text{ImTFSI}$, $C_2C_1\text{ImTFSI}$, $C_4C_1\text{ImTFSI}$, $C_6C_1\text{ImTFSI}$, and $C_8C_1\text{ImTFSI}$ [55]. Another hypothesis is that for geometrical reasons imidazolium cations find preferential paths of diffusion [76]. Figure 5.2 also shows that the difference between the self-diffusion of anions and cations is smaller for the protic ionic liquids, possibly due to strong ion-ion interactions and thus a more associative diffusional motion.

5.1.1 The effect of adding water

The main effect of adding water to ionic liquids is an enhanced diffusivity for all molecular species (**Paper I**). This is in agreement with a decreased self-diffusion activation energy as predicted by molecular dynamics simulations [77]. Figure 5.3 shows the normalized diffusivities of the cations (expressed as D^+/D_{neat}) and reveals a span of increases

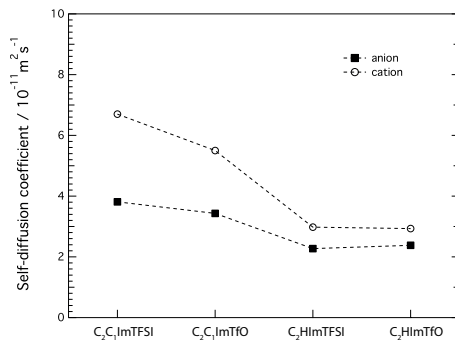


Figure 5.2: Self-diffusion coefficients measured at 30°C for the pure imidazolium ionic liquids investigated in this thesis.

in the self-diffusion, indicating that the molecular structure of the ions has an impact. More precisely the highest increase with respect to the pure ionic liquid is observed for C_2HImTfO (four-fold), followed by $\text{C}_2\text{HImTfSI}$, $\text{C}_2\text{C}_1\text{ImTfO}$ and $\text{C}_2\text{C}_1\text{ImTfSI}$.

The addition of water to the protic ionic liquid DEMA-OMs also results in an increase of self-diffusion (**Paper III**). However, the self-diffusion coefficients are lower than for imidazolium based ionic liquids, and similar for anions and cations in the entire concentration range investigated. Hence in this ionic liquid ions move more associatively than in imidazolium based protic ionic liquids.

5.1.2 The effect of adding imidazole

As opposed to the case of adding water, the effect of adding imidazole was exclusively investigated for the protic ionic liquid $\text{C}_2\text{HImTfSI}$. This choice was motivated by the fact that imidazole is capable of forming hydrogen bonds (hypothetically to the protic imidazolium cation) and the fact that TfSI is known to weakly coordinate to the cation (**Paper II**). The self-diffusion coefficient of the cation shows an overall increase with a complex dependence on the imidazole concentration (**Paper V**), see also Figure 5.9. It increases for mole fractions between 0 and 0.2 and above 0.6, while it has almost constant values between 0.2 and 0.6. Furthermore, the self-diffusion of the NH protons is greater than the

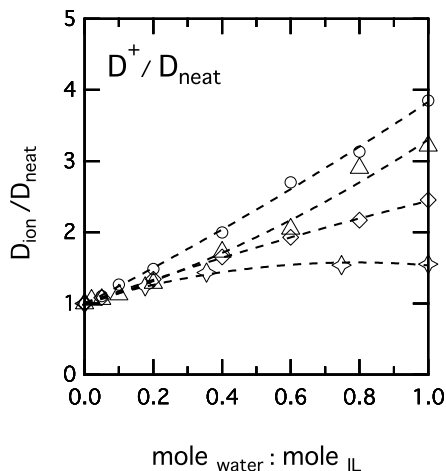


Figure 5.3: Normalized self-diffusion values, D^+/D_{neat} , for the cations in $C_2HImTfO$ (circles), $C_2HImTFSI$ (triangles), C_2C_1ImTfO (diamonds), and $C_2C_1ImTFSI$ (stars) as a function of added water.

molecular diffusion in the entire concentration range, suggesting the occurrence of structural diffusion with $-NH$ protons being dynamic and forming an extended hydrogen bonded network with the appropriate strength. A similar behavior was discussed for non-equimolar mixtures of imidazole and HTFSI as well as pyrazole and HTFSI [79].

5.2 Ionic conductivity

Figure 5.4 shows the ionic conductivity measured at 30 °C for the pure ionic liquids considered in this thesis. The conductivity of C_2C_1ImTfO and $C_2C_1ImTFSI$ (aprotic ionic liquids) is higher than that of $C_2HImTFSI$ and $C_2HImTfO$ (protic ionic liquids) (**Paper I**), which is attributed to a lower viscosity of these ionic liquids as compared to their protic counterparts. This can in turn be the result of weaker interaction between cations and anions. When water is added, the conductivity of all ionic liquids increases, Figure 5.5. This increase is moderate for $C_2C_1ImTFSI$ that shows almost constant values for concentrations above 0.2 due to phase separation. Its protic counterpart, $C_2HImTFSI$, displays phase separation at a higher concentration (*i.e.* at 0.8). This is attributed to

the hydrophobicity of the TFSI anion, that results in an only partial miscibility of TFSI based ionic liquids with water. The TfO anion, on the contrary, is more hydrophilic and increases the miscibility with water. The TfO based protic ionic liquid $C_2HImTfO$ shows the maximum conductivity value at 60 mS/cm. The OMs anion is also hydrophilic and miscible with water, however DEMA-OMs displays a lower ionic conductivity, which can be the result of a higher viscosity as compared to imidazolium based ionic liquids.

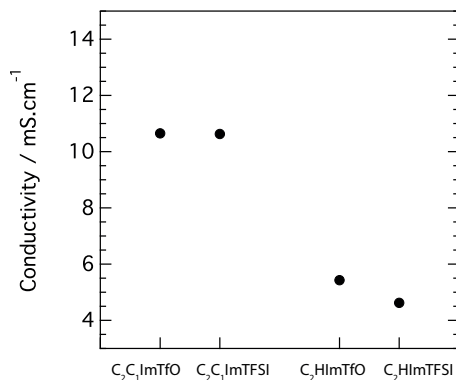


Figure 5.4: Ionic conductivity of the pure ionic liquids investigated in this thesis, measured at 30 °C.

Another interesting observation is that the ionic conductivity of the water miscible ionic liquids shows a bell-shape with a maximum value in the water-rich concentration range. This value marks a point where the decrease in ion concentration becomes more important than the increased mobility of the ions or their degree of dissociation (recall the equation 3.14). The universality of this behavior is a subject of debate that is currently being investigated both experimentally and computationally [80, 81].

From the conductivity and diffusivity of the ions, we could estimate the ionic dissociation in the binary systems of ionic liquids and water. The ionic dissociation (ionicity) was evaluated using the $\Lambda_{imp}/\Lambda_{NMR}$ ratio. The ratio is between 0.4 to 0.7 for all examined ionic liquid water mixtures, indicating that not all diffusing ionic species contribute to charge transfer (**Paper I** and **Paper III**). The ionicity in protic ionic liquids is lower than in aprotic ionic liquids, which may be a reflection

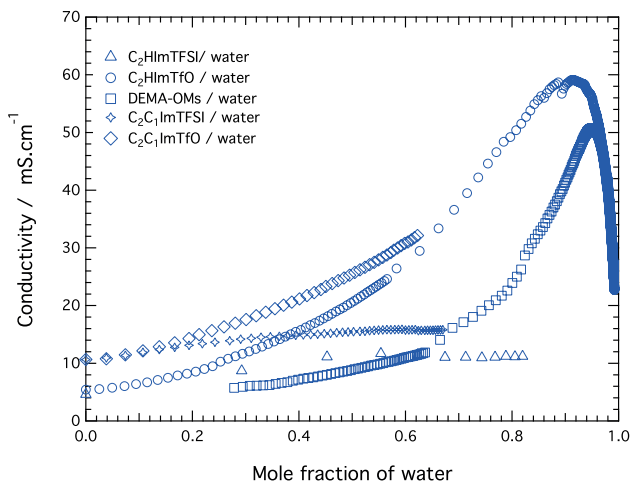


Figure 5.5: The ionic conductivity of the investigated ionic liquids as a function of water mole fraction measured at 30 °C.

of stronger cation-anion interactions. The ionicity, however, increases slightly upon addition of water, suggesting that water can interfere with the coulombic attraction between the ions. Nevertheless, in the aprotic ionic liquids $C_2C_1ImTFSI$ and C_2C_1ImTfO the ionicity is less affected by water. In DEMA-OMs the ionicity calculated based on diffusion coefficient measured at 25 °C (**Paper III**) shows an increase up to a water mole fraction of 0.3 but a decrease for higher water content. This shows that the interaction between cations and anions is disrupted at low water concentrations but may change at higher concentrations. In this case water may interact with two anions, as previously observed for other ionic liquids [82], and form a bigger molecular complex.

5.2.1 Adding water or ethylene glycol

We observed that the increase of ionic conductivity upon addition of water was larger for $C_2HImTfO$ than for $C_2HImTFSI$ or DEMA-OMs. Moreover, the proton exchange between water and $C_2HImTfO$ occurs at

a faster rate. This observations motivated us to investigate the mixture of $C_2HImTfO$ with ethylene glycol, which like water is capable of forming hydrogen bonds with the ionic liquid. Differently from water, however, ethylene glycol has a better thermal stability as also revealed by TGA experiments for the $C_2HImTfO$ /ethylene glycol mixtures (**Paper VII**). The addition of ethylene glycol has previously been examined only for aprotic ionic liquids wherefore there is very little information available on the behavior of protic ionic liquids when mixed with ethylene glycol [34, 83, 84].

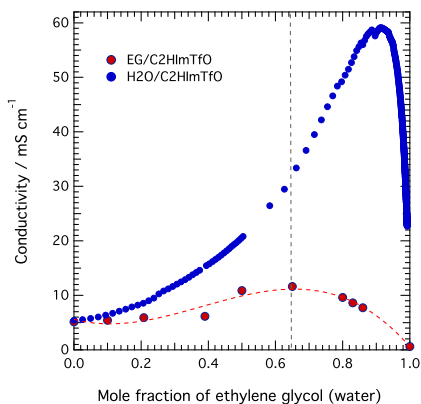


Figure 5.6: Conductivity of the binary mixture of $C_2HImTfO$ and ethylene glycol (red) and $C_2HImTfO$ and water (blue) as a function of water (or ethylene glycol) mole fraction measured at $30\text{ }^\circ\text{C}$.

The ionic conductivity of the $C_2HImTfO$ /ethylene glycol mixture is compared to that of a $C_2HImTfO$ /water binary system in Figure 5.6. The figure reveals that the conductivity is much less increased upon addition of ethylene glycol. However, TGA experiments reveal that the solution is stable up to approximately $120\text{ }^\circ\text{C}$ (**Paper VII**), which is a slight improvement with respect to the stability of water based electrolyte that are limited to below $100\text{ }^\circ\text{C}$. Furthermore, the Walden plot shows that the ionic dissociation of the mixture is improved by addition of ethylene glycol. The values are close to the ideal Walden behavior, which implies that the mixture represents the character of a 'good ionic liquid' with appropriate ionic dissociation properties, Figure 5.7. This can be rationalized by the marked decrease in viscosity (see Figure 5.11) accompanied by an increased ionic conductivity.

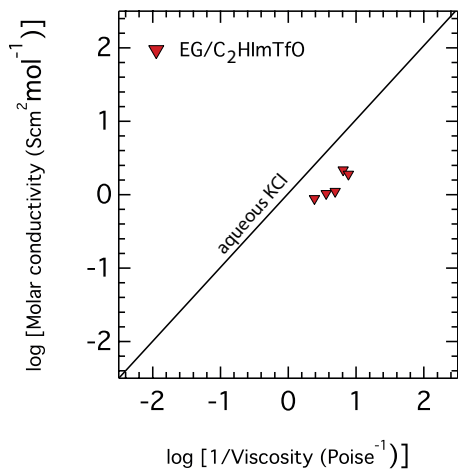


Figure 5.7: Walden plot for the binary mixture of ethylene glycol/ $C_2HImTfO$ reproduced from data obtained at $30^\circ C$.

5.3 Proton transfer

Proton exchange can occur in short-range or long-range distances within a material, Figure 5.8. The short-range type occurs back and forth between two adjacent molecules and will not necessarily result in proton deficient regions in the material. This is different from the long-range type of exchange, where the proton jumps from a proton excess site to a proton deficient site through a hydrogen bonded network. The latter is known as structural diffusion or 'Grotthuss mechanism' of proton transfer and in contrary to local proton exchange will result in higher diffusion coefficients of the protons. The proton transport in protic

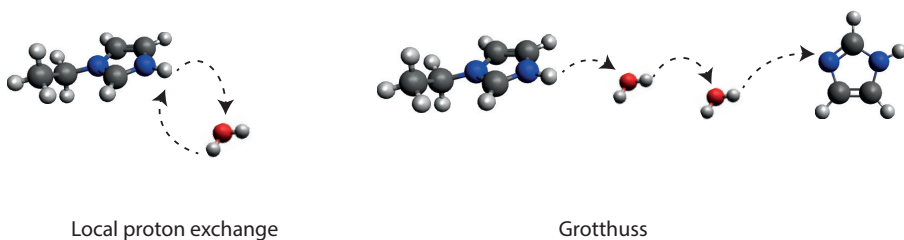


Figure 5.8: Short-range and long-range proton exchange.

ionic liquids can be mediated by the proton exchange between the –NH group of the cation and the second compound added to the ionic liquid. One purpose of adding water, ethylene glycol and imidazole to selected protic ionic liquids (*i.e.* C₂HImTFSI, C₂HImTfO and DEMA-OMs) was in fact to investigate this phenomenon.

By adding D₂O to the protic ionic liquid and subsequently analysing the ¹H NMR spectra we could estimate the rate of proton exchange in the protic ionic liquids C₂HImTFSI and C₂HImTfO. If the protons exchange, the ¹H NMR spectra show that the intensity of the –NH proton decreases while that of deuterated water increases (**Paper I**). Interestingly, the –NH proton resonance in C₂HImTfO merges with that of water and shifts to lower chemical shifts as the concentration of D₂O/water increases. This indicates that the proton exchange between deuterated water and C₂HImTfO occurs at a rate which is significantly higher than for C₂HImTFSI [85]. Further, the issue of proton transfer by Grotthuss mechanism was assessed by the D_{NH}/D_{cation} ratio. Our results indicate that the diffusivity of the –NH protons in C₂HImTFSI is not higher than that of the cations, suggesting that the proton transfer in this system is not conform to the Grotthuss mechanism. The D_{NH}/D_{cation} ratio could not be analyzed for C₂HImTfO due to the merged character of the –NH and the water proton resonances.

Having learned that the proton exchange in water and C₂HImTFSI is slower, making the NH and water proton resonances distinct and available for diffusion measurements, we chose this ionic liquid to add imidazole and closely investigate the proton exchange between the cation and added imidazole (**Paper V**). We observed that the D_{NH}/D_{cation} ratio is systematically higher than unity, Figure 5.9. As a consequence the self-diffusion coefficient of the NH group (D_{NH}) can be assumed to contain the contribution from the vehicular (D_{cation}) and the Grotthuss (D_{H^+}) mechanisms through the relation:

$$D_{NH} = \chi D_{H^+} + (1 - \chi) D_{cation}$$

where χ is the mole fraction of added imidazole. The calculated D_H values display a dependence on composition and a minimum at $\chi \simeq 0.5$. This observation together with results obtained experimentally and computationally from MD simulations, let us conclude that to some extent the Grotthuss mechanism does contribute to the overall charge

transport, as opposed to the case of pure $C_2HImTfSI$ and of the water/ $C_2HImTfSI$ mixtures (**Paper I**).

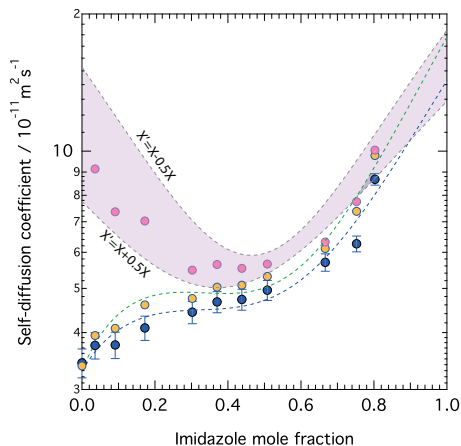


Figure 5.9: Self-diffusion coefficients measured at 30 °C for the imidazolium cation (D_{cat} , blue) and the proton bound to the nitrogen atom (D_{NH} , yellow) as a function of composition. Pink symbols represent the D_H values obtained from Eq.(5.3).

5.4 Density and viscosity

The effect of adding water, ethylene glycol and imidazole was also examined with respect to density and viscosity. Figure 5.10 shows that in all systems the addition of the second compound results in a reduced density. This implies a lower excess molar volume and as previously observed indicates that the number of hydrogen bonds between the second component and the ionic liquid is increased [18]. It is interesting to note that the effect of water on density is stronger than that of ethylene glycol when mixed with $C_2HImTfO$, while in $C_2HImTfSI$ the addition of imidazole and water have similar effects. This is certainly due to the way ions and added compounds interact with each other.

The viscosity of the binary mixtures $Im/C_2HImTfSI$ and $EG/C_2HImTfO$ is presented in Figure 5.11. The overall effect is a decreased viscosity that results in increased self-diffusion coefficients in both systems, see also section 3.1 and **Paper VII**. The trend observed for ethylene glycol/ $C_2HImTfO$ is in agreement with that previously reported for

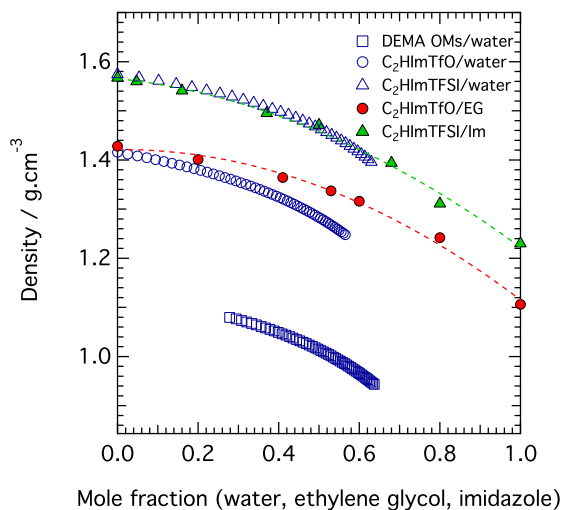


Figure 5.10: Density variation in protic ionic liquids as a function of added water, ethylene glycol and imidazole.

other protic ionic liquids like PyrrHSO_4 and $\text{PyrrCF}_3\text{COO}$ [86]. The change in viscosity for the $\text{Im}/\text{C}_2\text{HImTFSI}$ is less pronounced than for ethylene glycol/ C_2HImTfO .

Mixing ionic liquids with water or imidazole has also effects on the thermal properties. The glass transition temperature (T_g), if observed, and the melting temperature (T_m) are presented as a function of composition in Figure 5.12. The melting point of the aprotic ionic liquids $\text{C}_2\text{C}_1\text{ImTFSI}$ and $\text{C}_2\text{C}_1\text{ImTfO}$ is lower due to the larger size and lower symmetry of the cation as compared to their protic analogues, and weaker cation-anion interactions (*e.g.* numbers of hydrogen bonds). Moreover, the melting point of all examined ionic liquids (except for the $\text{C}_2\text{C}_1\text{Im-TFSI/water}$) decreases upon addition of a second compound. This can be attributed to a drastic change in ion-ion coordination and consequently the disruption of the effective packing of the ions even at very low concentrations of the added compound. The effect on T_m depends on both the initial strength of ion-ion interactions as well as the possible interaction established between ions and the second compound. For example, in $\text{C}_2\text{C}_1\text{ImTFSI}$ the TFSI anion is hydrophobic and less affine to form hydrogen bonds with water. The $\text{C}_2\text{C}_1\text{Im}$ cation

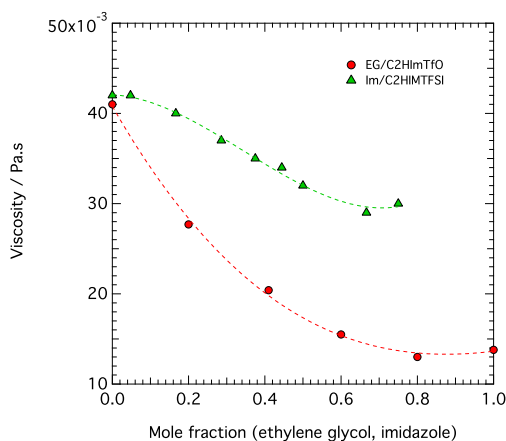


Figure 5.11: *Viscosity variation in protic ionic liquids as a function of added ethylene glycol and imidazole.*

also does not form strong hydrogen bonds with water, therefore the mixture of $C_2C_1ImTfSI$ and water is miscible with water only up to $x_{water}=0.2$ and phase separates. The TfO anion on the other hand is more hydrophilic and by forming hydrogen bonds with water also results in more evident changes in T_m . The new hydrogen bond with water weakens the hydrogen bond between cation and anion and induces a disorder which can be clearly seen as a drop in the melting temperature of the mixture. The decrease in T_g is assigned to a 'plasticizing' effect of water. A decrease in T_g is generally beneficial because it results in lower viscosity at a comparable high temperature (and thus faster molecular dynamics), while lower values of T_m enlarge the liquid window extending to well below room temperature. These new properties are favorable from fuel cell applications if use at extreme weather conditions is considered.

5.5 Intermolecular interactions

The 1H NMR chemical shift as well as the frequency of some molecular vibrations of the studied ionic liquids are sensitive to the chemical environment of the molecules. The infrared frequencies of the C-H and N-H stretching and the chemical shift of 1H resonances are good probes for

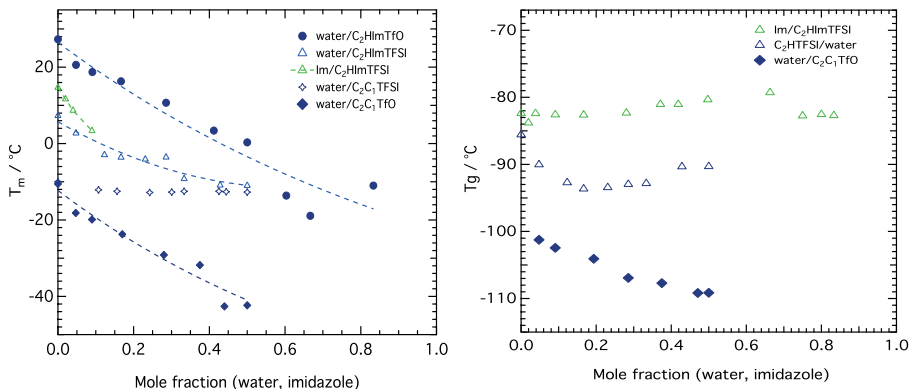


Figure 5.12: Melting point (left) and glass transition temperature (right) of examined ionic liquids as a function of water/imidazole.

the chemical environment of the cation, while Raman spectroscopy is more suitable to study the state of the anions. In the case of changes in the hydrogen bond configurations the chemical shift of the protons involved shift down-field. Figure 5.13 presents the change in the chemical shift of the protic protons on the cation and that of the added compounds (*i.e.* OH of water and ethylene glycol).

In pure protic ionic liquids the chemical shift of the NH proton in $C_2HImTfO$ is more down-field than for $C_2HImTFSI$. This can be attributed to the degree of proton transfer from the HTFSI acid to ethylimidazole when they react to form a protic ionic liquid, as discussed recently by Davidowski *et al.* [87]. They have also shown that the protic ionic liquids that form through a weak proton transfer display lower ionicity [87]. This is consistent with our observation that the ionicity of pure $C_2HImTfO$ is lower than pure $C_2HImTFSI$ (**Paper I**), indicating a weaker proton transfer in $C_2HImTfO$ as compared to $C_2HImTFSI$ and the proton of the NH group is less shielded by the electron pairs of nitrogen.

Upon addition of a second component, we observed an increase in the chemical shift of the NH protons for the water/ $C_2HImTFSI$ (**Paper I**), Im/ $C_2HImTFSI$ (**Paper V**) and ethylene glycol/ $C_2HImTfO$ (**Paper VII**) systems. This shows that these protons are less shielded by

the electron pairs of the nitrogen, which is believed to be the result of the formation of stronger hydrogen bonds between the NH proton and the added compound. On the other hand, the decreased chemical shift observed for the protons of water or of the imidazolium cation in water/C₂HImTFSI and Im/C₂HImTFSI implies that these protons are more shielded as a result of being surrounded by alike molecules. We also observed an increase in the chemical shift of the OH protons of ethylene glycol in ethylene glycol/C₂HImTfO (**Paper VII**), and OH of water in water/DEMA-OMs (**Paper III**), which indicates that these protons also are being involved in stronger hydrogen bonds as the concentration increases. This can be attributed to the affinity of the TfO and OMs anions to form hydrogen bond with ethylene glycol or water.

We have also observed an anomaly in Im/C₂HIMTFSI in the chemical shift change of the NH proton that shows a strong non-linear dependence on composition (**Paper V**), indicating that the protic site, shared between the imidazolium cation and imidazole, experiences progressively stronger hydrogen bonds. The deviation from an ideal trend is maximum at $\chi=0.5$, (Figure 5.13), a composition that corresponds to a decreased contribution of the Grotthuss mechanism of proton transfer.

Infrared spectroscopy also provides information about different coordinations between the cation and the added compound in the investigated binary systems. In water/imidazolium based protic ionic liquids, the frequency of NH group remains almost unaltered in C₂HImTFSI upon addition of water while that in C₂HImTfO reveals a red-shift and indicates a hydrogen bonded structure. We also detected a feature in C₂HImTFSI spectra at 917 cm⁻¹ that grows upon addition of water, which we tentatively attribute to the out of plane bending mode (γ) of the -NH group. Moreover, two other growing features at 820 and 905 cm⁻¹ presumably relate to the interaction between water and the C²H and N³H groups of the cation, with water possibly sharing its oxygen between these sites (see Figure 5.14). The effect on the state of the anion is explored by Raman spectroscopy which reveals that the TFSI anion is barely affected by the presence of water while the S–O and the C–S stretching modes of TfO shift to higher frequencies indicating a stronger coordination between anions and water. These observations indicate that in C₂HImTfO water coordinates to both cation and anion, while in C₂HImTFSI it coordinates mainly to the cation, Figure 5.14.

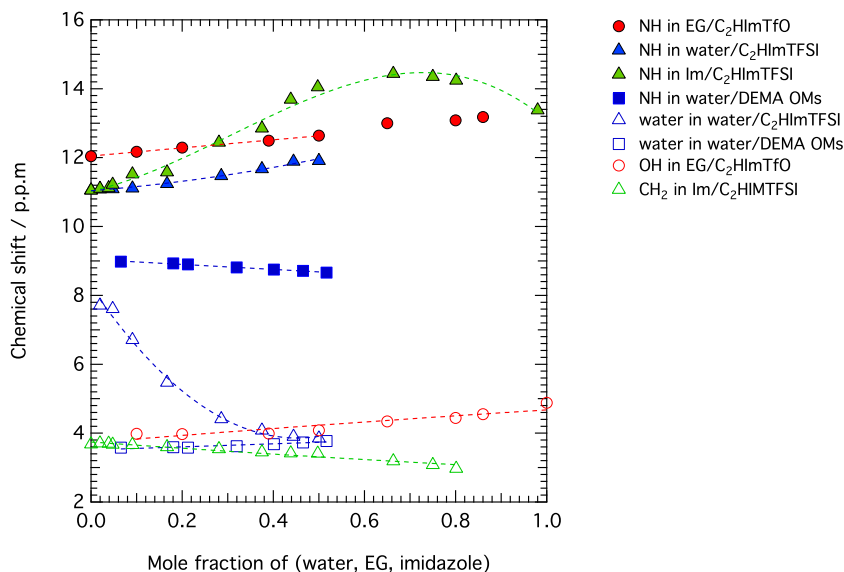


Figure 5.13: The variation of the chemical shift of NH proton of the protic ionic liquid and that of the added substance as a function of mole fraction of the added compound.

Our infrared analysis for the DEMA-OMS system reveals that the frequency of the N-H stretching mode blue-shifts with increasing water content, differently from the case of imidazolium based ionic liquids. This suggests that water mainly coordinates to the OMs anion and liberates the cation despite it also possesses a NH group with a potential to form hydrogen bonds. The Raman spectra also show a red-shift of the C-S and S-O stretching modes of the OMs anion, confirming the hypothesis of stronger interaction between the anion and water (**Paper III**).

In the Im/C₂HImTFSI system the infrared spectra analysis also confirms that the NH sites (NH⁺ of imidazolium and NH⁰ of imidazole) do participate in an extended hydrogen bonded network, which is concentration dependent. Up to $\chi=0.2$ both NH⁺ and NH⁰ experience stronger hydrogen bonds (red shift), which is plausibly due to increased (in number or strength) NH⁺...NH⁰...TFSI interactions. In the 0.2–0.5 range, however, the imidazolium relaxes back to shorter N-H⁺ bonds (blue shift and weaker NH...bonds), while the frequency of the N-

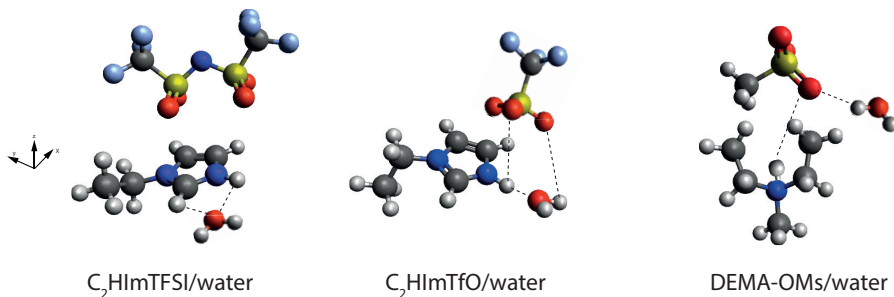


Figure 5.14: *The schematic illustration of coordination of water molecule toward cation/anion in investigated protic ionic liquids.*

H^0 stretching (in imidazole) further red shifts displaying a continued trend towards stronger $\text{NH}^0 \cdots$ bonds. For $\chi > 0.5$ both N-H^+ and N-H^0 stretching frequencies show a blue shift and thus a tendency towards overall weaker hydrogen bonds. This trend reveals a competition between ion-ion and ion-imidazole interactions, which may lay behind the composition dependence of both the ionic self-diffusion and the proton transfer by the Grotthuss mechanism. The local coordination of TFSI is revealed by Raman spectroscopy, which shows an overall downshift of the characteristic mode at 742 cm^{-1} and a weaker interaction between the anions and surrounding molecules upon addition of imidazole. These observations can be rationalised by a transition from an ionic network stabilised by mainly Coulombic forces in pure $\text{C}_2\text{HImTFSI}$ to interactions of strong hydrogen bond character in the imidazole-rich composition (**Paper V**).

The infrared analysis of the ethylene glycol/ C_2HImTfO system shows that the OH stretching mode of ethylene glycol shifts to lower wavenumber as a result of progressively stronger hydrogen bonds. The NH stretching mode, however, is very hard to analyse due to a strong overlap with the OH stretching modes. Nevertheless, the chemical shift of the NH proton reveals that the cation also experiences strong hydrogen bonds as the concentration of ethylene glycol increases. Upon addition of ethylene glycol the SO_3 stretching mode shifts to lower frequencies, indicating that the S–O bond is more elongated and may form hydrogen bond with ethylene glycol (**Paper VII**).

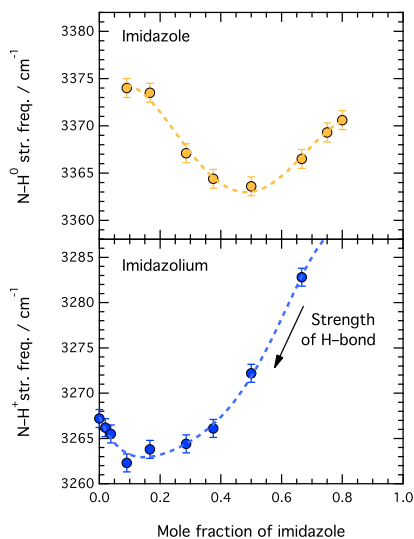


Figure 5.15: Composition dependence of the $N-H^0$ (imidazole) and $N-H^+$ (imidazolium) stretching frequencies as obtained by peak fit analysis of the infrared spectra.

5.6 The effect of nano-confinement

In **Paper IV** we have incorporated the hydrated protic ionic liquid (DEMA-OMS) in nano-porous silica micro-particles to study the effect of nano-confinement on dynamics and local coordination. Hereafter, the product of the mixing is called 'gel'. NMR analyses show that the silica surface is covered with water molecules, which are strongly bonded and show a very limited mobility. Raman spectroscopy reveals that water disrupts the classic cation-anion interaction, while 2D solid-state NMR shows that the cations closer to the surface adopt a preferred coordination with the NH^+ group oriented towards silica.

Diffusion NMR shows that nano-confinement does not affect the mobility of the ions drastically. This is partly explained by the screening effect of water adsorbed at the silica surface. A comparison between this type of gel with imidazolium based gels previously reported [50] shows that the apparent self-diffusion coefficient is higher, partly also due to a lower surface area and thus less surface interactions.

In **Paper VI** we have investigated the effect of surface functionalization by hydrophobic butyl groups. Two ionic liquids, one protic (DEMA-OMs) and one aprotic ($C_6C_1ImTFSI$) were incorporated into functionalized nano-porous silica micro-particles. The results show an overall enhanced ionic mobility, in particular in the nano-confined condition as a result of decreased ionic liquid-silica interactions. The conductivity of both ionic liquids in functionalized particles is systematically higher than in untreated particles. In addition, the ionic conductivity drop as compared to the bulk state is less pronounced than that in covalently bound gels (organic or inorganic), see Figure 4 in **Paper VI** .

Overall, nano-porous silica provides sufficient volume for holding the ionic liquid and can serve as a support material for electrolytes to be used in energy relevant devices such as fuel cells. In addition, by tuning the surface chemistry of the pore walls enhanced transport properties can be achieved. This can be useful for other applications where mass transfer through a porous network is crucial.

Concluding remarks and future outlook

This thesis was focused on understanding the effect of adding a neutral molecule on the dynamics and intermolecular interactions in protic ionic liquids. I believe that this work has provided useful information for the design of new electrolytes based on binary mixtures of protic ionic liquids, a field of materials science that needs to be further explored.

The findings of this thesis show that diffusion NMR as well as ^1H NMR and vibrational (Raman and infrared) spectroscopy are useful and reliable techniques for investigating the dynamics and the molecular interactions in these liquid systems. However, it is worth noting that NMR diffusometry becomes challenging for measurements at high temperatures due to the effect of convection that may lead to a wrong estimation of the self-diffusion coefficients. To study the translational motion at high temperatures, other techniques such as Quasi-Elastic Neutron Scattering (QENS) would be more suitable. Compared to diffusion NMR, QENS experiments also allow to cover a much wider time range extending down to the picoseconds regime.

Our results show that *hydrated* ionic liquids display better diffusive and conductive properties than the pure or *anhydrous* liquids. Cations and anions, however, can be affected differently and by an extent that depends on their hydrophilicity/hydrophobicity and their ability to form hydrogen bonds with water. The protic ionic liquid C_2HImTfO showed to be the most affected ionic liquid since water coordinates to both the

TfO anion and the C₂HIm cation by establishing direct hydrogen bonds with the protic site of the cation and the oxygens of the anion. This is also reflected in a faster proton exchange between the cation and water as compared to the case of C₂HImTFSI where the water forms non-directional hydrogen bonds only with the cation. Although apparently subtle, this distinct behavior can be a useful insight to design new electrolytes with a promoted proton transfer. A future work of relevance could be estimation of the Grotthuss contribution to the overall proton transport in C₂HImTfO/water mixtures by means of QENS as a function of both temperature and water concentration.

Proton transfer through the Grotthuss mechanism was observed in imidazole/C₂HImTFSI mixtures, mainly at low imidazole concentrations. Because of the properties of the TfO anion as compared to TFSI, an interesting system to investigate should be the mixture of imidazole and C₂HImTfO, which may possibly show a fast proton motion in the whole concentration range. Further, other cationic structures may be considered in the future, for example cations derived from pyrazole. A lot remains to do for what concerns the behaviour of pure or mixed protic ionic liquids when confined in a solid porous material that can provide non-leakage, as required for use in fuel cells. Solid gels supported by nano-porous silica micro-particles represent one approach in this direction (and the one investigated in this thesis) but other organic or inorganic networks may serve equally well for the retention of protic ionic liquid based electrolytes. What we underline is that the ionic or proton mobility can be tuned by controlling the surface chemistry of the pore walls that contain the liquid phase. One suggestion for future gel electrolytes is to incorporate a suitable mixture of imidazole and C₂HImTFSI or imidazole and C₂HImTfO inside hydrophobic nano-porous silica particles as those investigated in this thesis, or silica particles grafted with proton donating groups such as phosphonic (H₂PO₄) or sulphonic (HSO₄) acids. Another suggestion for future work is to perform fuel cell tests for these materials and evaluate their performance in real operational condition.

Acknowledgements

The financial support from the Chalmers' *Energy* Area of Advance is kindly acknowledged.

I would also like to express my gratitude to the following people:

My supervisor **Assoc. Prof. Anna Martinelli** for your great supervision and support during these years. I am very proud for being your first PhD student. In addition to all trust that I have on you for work related issues and scientific matters you have been a great role model for me as a knowledgeable hard-working woman scientist in academia. I will miss you and our mystery solving moments. I also would like to thank **Assoc. Prof. Lars Nordstierna** my co-supervisor for your supervision on NMR spectroscopy related issues, all scientific discussions, kindness and your great support throughout these years.

My examiner, **Prof. Anders Palmqvist** for giving me the opportunity to work in 'Diamond 2160' division to learn how to be a good researcher and also a better person.

My co-authors, **Prof. Aleksandar Matic, Dr. Jagath Pitawala,**

Luis Aguilera, and **Prof. Michael Persson** for all fruitful discussions and collaborations. The same goes to **Dr. Victor V. Gómez González** and **Prof. Luis M. Varela Cabo** for performing molecular dynamics simulations and **Prof. Elisabeth Ahlberg** and **Adriano Gomez** for the work on Cr_2O_3 nanoparticles.

To **Dr. Romain Bordes** for your help and support in many things from lab related issues to parenting matters. I would like also to thank **Dr. Anna Ström** for being very kind to me and assisting me in viscosity measurements. **Prof. Johan Bergeholtz** for his generous permission to use the instruments for density and viscosity measurements.

Special thanks to **Moheb** and **Mounesha** my former research group colleagues. It was fun to work with you and I have always greatly enjoyed your company.

My former roommates **Marina** and **Alexander** and current roommate **Frida**. How lucky I have been to meet you guys! Your positive mindset and problem solving attitude have always delighted my soul.

Prof. Göran Karlsson and colleagues at **Swedish NMR centre** for providing infrastructure for diffusion NMR measurements. Special thanks to **Dr. Diana Bernin** for her great support in NMR experiment 'frustration moments' whenever I needed.

Mattias and **Amaia** for their great help with DSC and TGA instruments, keeping them up and running!

Dear **Ann** for all administrative work and also your invaluable support during the years I spent at Chalmers.

My former and present **colleagues and friends at TYK and KCK and polymer chemistry**, Caroline, Anand, Sanna, Johanna, Adele,

Milene, Simon, Emma, Ting, Leo, Peter, Anne, Saba for your great company and creating a very nice working atmosphere. Samuel and Giulio special thanks to you for your care and support in last days of writing my thesis. You lifted my spirit!

My dear **Parents**, sisters and brother **Negar, Golnaz, Mohammad** and my dear friends **Arghaven, Masoud** and **Nargess** for your endless love, support and encouragements.

Farshid, for providing peace and quiet for Raha at home when I was away.

And my 'sweetest devotion' **Raha** who enlivens my life with joy, hope, happiness and wonder, day by day. We have started this journey together from the very beginning. I love you so much!

8.1 The fuel cell technology

The fuel cell is an electrochemical device in which the chemical energy is released from oxidation of hydrogen at the anode and reduction of oxygen at the cathode to produce electricity, water, and heat [27]. Basically, fuel cells can be divided into different types according to their working temperature, electrolyte used, and consumed fuel. These are described in more details below.

In Figure 8.1 different types of fuel cells are schematically shown.¹ Solid oxide fuel cells (SOFC) operate at high temperatures, typically between 700 and 1000 °C. The electrolyte is a solid ceramic consisting of yttria-stabilized zirconia, and the overall efficiency can reach 80 percent if heat is recovered. SOFCs are resistant to impurities of the fuel such as carbon monoxide and sulfur and can use a variety of hydrocarbons as the fuel. Molten carbonate fuel cells (MCFC) are also working at high temperatures, 600 - 700 °C, with fuel-to-electricity conversion efficiency up to 60 percent. Another class of fuel cells are alkaline fuel cell, in which hydroxyl groups (OH^-) react with hydrogen at the anode. The operating temperature is between 90 to 100 °C and the efficiency is about 60-70 percent. Phosphoric acid fuel cells (PAFC) use phosphoric acid as the electrolyte and have an optimal operating temperature between

¹Reproduced from:<http://www.fuelcells.org>

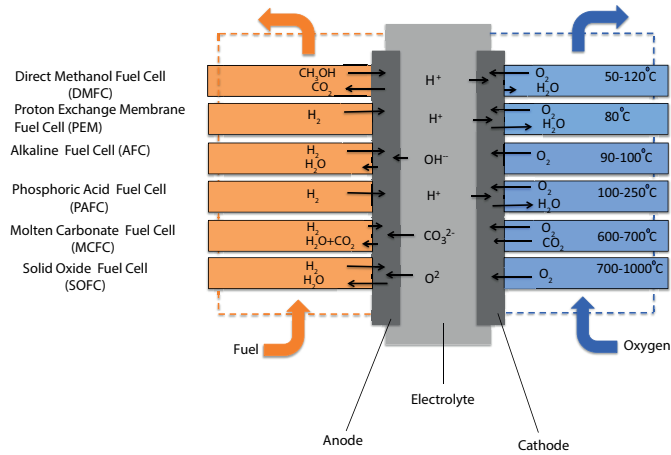


Figure 8.1: Different types of fuel cells, categorized based on the electrolyte and the working temperature.

180 and 210 °C, and an electrical efficiency of about 70 percent [88].

Currently, the best developed fuel cells are proton exchange membrane fuel cells (PEMFC), also known as polymer electrolyte membrane fuel cells. The working temperature is below 100 °C and the fuel-to-electricity conversion efficiency is between 40–60 percent. Due to safety concerns about hydrogen storage and transport in vehicles, direct methanol fuel cell (DMFC) was later developed. DMFC is a polymer membrane fuel cell but methanol (CH_3OH) is used as the fuel instead of hydrogen (H_2). In DMFC hydrogen is drawn from methanol using a platinum-ruthenium catalyst. The operation temperature of DMFCs is between 50 and 120 °C. Differently from hydrogen, methanol can be stored or transported more safely. However, a drawback of DMFC is the methanol crossover through the electrolyte [88].

8.2 The proton exchange membrane fuel cell

The proton exchange membrane fuel cell (PEMFC) was first developed and demonstrated by General Electric as an auxiliary power source for a NASA space program in the 1950s [89]. Today’s PEMFC versions use

an acidic polymer membrane, typically Nafion, as the electrolyte, and carbon based electrodes loaded with platinum nano-particles. Nafion is a copolymer consisting of tetrafluoroethylene and sulfonated head groups. When hydrated, the sulfonic acid head groups ($-\text{SO}_3\text{H}$) dissociate and release mobile protons. The protons become charge carriers and diffuse through the membrane assisted by the aqueous medium. Simultaneously the remaining $-\text{SO}_3$ groups are hydrated/shielded by water at the polymer-water interface [90], Figure 8.2. Due to the low operational temperature, the PEMFC have been implemented more in backup power units than in vehicles up to now.

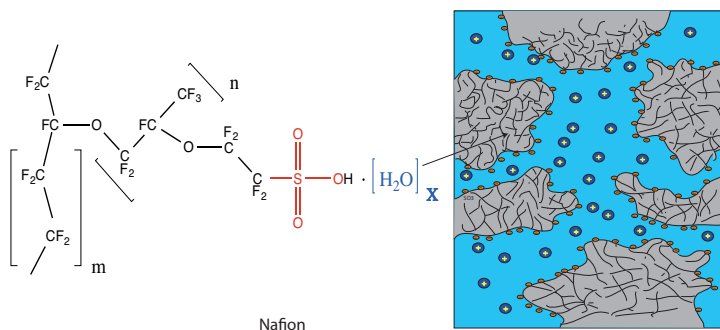
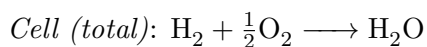
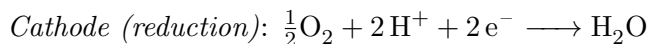
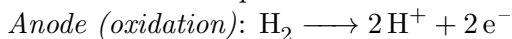


Figure 8.2: Molecular structure of Nafion (left) and separation into hydrophobic (gray) and hydrophilic (blue) nano-domains (right).

As shown in Figure 8.3, hydrogen splits into protons on the surface of the platinum catalyst at the anode side, while the electrons are directed to an external circuit and the protons are transported through the membrane to react with electrons and oxygen at the cathode where heat and water are produced. The reactions are summarized as follows:



The most important issue in a PEMFC is the operational temperature,

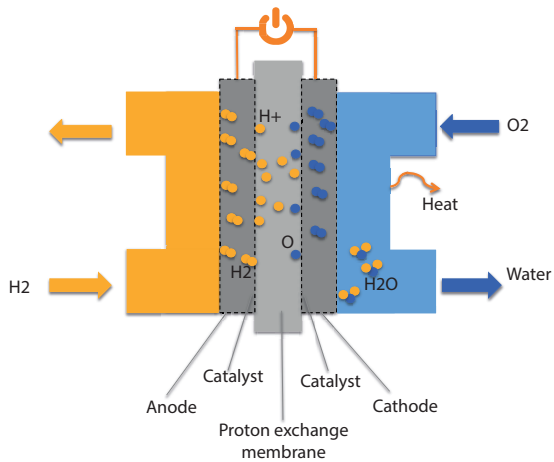


Figure 8.3: *How a PEM Fuel cell works.*

which has to be below $100\text{ }^\circ\text{C}$ to maintain the membrane's humidity. Evaporation of water at temperatures above $100\text{ }^\circ\text{C}$ affects negatively the fuel cell's overall performance, as reflected by the drastic decrease of proton conductivity [28]. On the other hand, higher operational temperatures enhance the CO-tolerance of platinum, that is otherwise very sensitive to CO poisoning.

Bibliography

- [1] UNECE. Climate Change and Sustainable Transport.
- [2] Mariana Diaz, Alfredo Ortiz, and Inmaculada Ortiz. Progress in the use of ionic liquids as electrolyte membranes in fuel cells. *Journal of Membrane Science*, 469:379–396, 2014.
- [3] Negin Yaghini, Jagath Pitawala, Aleksandar Matic, and Anna Martinelli. Effect of water on the local structure and phase behavior of imidazolium-based protic ionic liquids. *The Journal of Physical Chemistry B*, 119(4):1611–1622, 2015.
- [4] Yuki Kohno and Hiroyuki Ohno. Ionic liquid/water mixtures: from hostility to conciliation. *Chemical Communications*, 48(57):7119–7130, 2012.
- [5] Michel Armand, Frank Endres, Douglas R MacFarlane, Hiroyuki Ohno, and Bruno Scrosati. Ionic-liquid materials for the electrochemical challenges of the future. *Nature Materials*, 8(8):621–629, 2009.
- [6] Paul Walden. Molecular weights and electrical conductivity of several fused salts. *Bull. Russian Acad. Sci.*, pages 405–422, 1914.
- [7] C. Austen Angell, Younes Ansari, and Zuofeng Zhao. Ionic Liquids: Past, present and future. *Faraday Discussions*, 154(1):9–27, 2012.

- [8] Hiroyuki Tokuda, Seiji Tsuzuki, Md Abu Bin Hasan Susan, Kikuko Hayamizu, and Masayoshi Watanabe. How ionic are room-temperature ionic liquids? An indicator of the physicochemical properties. *Journal of Physical Chemistry B*, 110(39):19593–19600, 2006.
- [9] Richard T. Carlin and John S. Wilkes. Complexation of Cp_2MgCl_2 in a chloroaluminate molten salt: relevance to homogeneous Ziegler-Natta catalysis. *Journal of Molecular Catalysis*, 63(2):125–129, 1990.
- [10] J. A. Boon, R. T. Carlin, A. M. Elias, and J. S. Wilkes. Dialkylimidazolium-sodium chloroaluminate ternary salt system: phase diagram and crystal structure. *Journal of Chemical Crystallography*, 25(2):57–62, 1995.
- [11] Wu Xu, Emanuel I Cooper, and C.A. Angell. Ionic Liquids: Ion Mobilities, Glass Temperatures, and Fragilities. *The Journal of Physical Chemistry B*, 107(25):6170–6178, 2003.
- [12] Robin D Rogers and Kenneth R Seddon. Ionic Liquids: Solvents of the Future? *Science*, 302(5646):792–793, 2003.
- [13] Peter Wasserscheid and Wilhelm Keim. Ionic Liquids - New Solutions for Transition Metal Catalysis. *Angew Chem Int*, 39:3772 – 3789, 2000.
- [14] Tomohiro Yasuda and Masayoshi Watanabe. Protic ionic liquids: Fuel cell applications. *Mrs Bulletin*, 38(7):560–566, 2013.
- [15] John S. Wilkes, Joseph A. Levisky, Robert A. Wilson, and Charles L. Hussey. Dialkylimidazolium chloroaluminate melts: a new class of room-temperature ionic liquids for electrochemistry, spectroscopy and synthesis. *Inorganic Chemistry*, 21(3):1263–1264, 1982.
- [16] Pierre Bonhôte, Ana-Paula Dias, Michel Armand, Nicholas Papageorgiou, Kuppuswamy Kalyanasundaram, and Michael Grätzel. Hydrophobic, Highly Conductive Ambient-Temperature Molten Salts. *Inorganic chemistry*, 35(5):1168—1178, 1996.
- [17] Tomohiro Yasuda, Hiroshi Kinoshita, Muhammed Shah Miran, Seiji Tsuzuki, and Masayoshi. Watanabe. Comparative Study on

- Physicochemical Properties of Protic Ionic Liquids Based on Allylammonium and Propylammonium Cations. *Journal of Chemical & Engineering Data*, 58(10):2724–2732, 2013.
- [18] Tamar L. Greaves and Calum J. Drummond. Protic Ionic Liquids: Evolving Structure-Property Relationships and Expanding Applications. *Chemical Reviews*, 115(20):11379–11448, 2015.
- [19] Kosuke Izutsu. History of the use of nonaqueous media in electrochemistry. *Journal of Solid State Electrochemistry*, 15(7-8):1719–1731, 2011.
- [20] Lynnette A. Blanchard and Joan F. Brennecke. Recovery of Organic Products from Ionic Liquids Using Supercritical Carbon Dioxide. *Industrial & Engineering Chemistry Research*, 40(11):2550–2550, 2001.
- [21] Joan F. Brennecke and Edward J. Maginn. Ionic liquids: Innovative fluids for chemical processing. *AIChE Journal*, 47(11):2384–2389, 2001.
- [22] Barbara Kirchner, Bronya Clare, Ralf Giernoth, Margarida F. Costa Gomes, José N. Canongia Lopes, Douglas R. MacFarlane, Anja-Verena Mudring, Agílio A. H. Padua, Mathieu Pucheault, Annegret Stark, Amal Sirwardana, Suzie Su Yin Tan, Andreas Taubert, and Michel Vaultier. *Topics in Current Chemistry-Ionic Liquids*. Springer, 2009.
- [23] Masahiro Yoshizawa, Wu Xu, and C Austen Angell. Ionic liquids by proton transfer: vapor pressure, conductivity, and the relevance of ΔpK_a from aqueous solutions. *Journal of the American Chemical Society*, 125(50):15411–15419, 2003.
- [24] Hiroyuki Tokuda, Kikuko Hayamizu, Kunikazu Ishii, Md Abu Bin Hasan Susan, and Masayoshi Watanabe. Physicochemical properties and structures of room temperature ionic liquids. 1. Variation of anionic species. *Journal of Physical Chemistry B*, 108(42):16593–16600, 2004.
- [25] Kazuhide Ueno, Hiroyuki Tokuda, and Masayoshi Watanabe. Ionicity in ionic liquids: correlation with ionic structure and physicochemical properties. *Physical Chemistry Chemical Physics*, 12(8):1649–1658, 2010.

- [26] Tamar L. Greaves and Calum J. Drummond. Protic ionic liquids: Properties and applications. *Chemical Reviews*, 108(1):206–237, 2008.
- [27] Stanley Angrist. *Direct Energy Conversion*. Allyn and Bacon Inc., Boston, 1965.
- [28] James R. O’Dea, Nicholas J. Economou, and Steven K. Buratto. Surface morphology of nafion at hydrated and dehydrated conditions. *Macromolecules*, 46(6):2267–2274, 2013.
- [29] Hirofumi Nakamoto, Akihiro Noda, Kikuko Hayamizu, Satoshi Hayashi, Hiro O. Hamaguchi, and Masayoshi Watanabe. Proton-conducting properties of a brønsted acid-base ionic liquid and ionic melts consisting of bis(trifluoromethanesulfonyl)imide and benzimidazole for fuel cell electrolytes. *Journal of Physical Chemistry C*, 111(3):1541–1548, 2007.
- [30] Akihiro Noda, Md Abu Bin Hasan Susan, Kenji Kudo, Shigenori Mitsushima, Kikuko Hayamizu, and Masayoshi Watanabe. Brønsted acid-base ionic liquids as proton-conducting nonaqueous electrolytes. *Journal of Physical Chemistry B*, 107(17):4024–4033, 2003.
- [31] T. J. Simons, P. M. Bayley, Z. Zhang, P. C. Howlett, D. R. Macfarlane, L. A. Madsen, and M. Forsyth. Influence of Zn^{2+} and water on the transport properties of a pyrrolidinium dicyanamide ionic liquid. *Journal of Physical Chemistry B*, 118(18):4895–4905, 2014.
- [32] Paul M Bayley, a S Best, D R MacFarlane, and M Forsyth. The effect of coordinating and non-coordinating additives on the transport properties in ionic liquid electrolytes for lithium batteries. *Physical Chemistry Chemical Physics*, 13(10):4632–4640, 2011.
- [33] Gitanjali Rai and Anil Kumar. Interesting thermal variations owing to cationic ring structural features in protic ionic liquids. *Physical Chemistry Chemical Physics*, 15(21):8050–8053, 2013.
- [34] Gitanjali Rai and Anil Kumar. Elucidation of Ionic Interactions in the Protic Ionic Liquid Solutions by Isothermal Titration Calorimetry. *The Journal of Physical Chemistry B*, 118:4160–4168, 2014.

- [35] Yuki Kohno and Hiroyuki Ohno. Ionic liquid/water mixtures: from hostility to conciliation. *Chemical Communications*, 48(57):7119–7130, 2012.
- [36] Robert Hayes, Silvia Imberti, Gregory G. Warr, and Rob Atkin. How water dissolves in protic ionic liquids. *Angewandte Chemie - International Edition*, 51(30):7468–7471, 2012.
- [37] Stefan Zahn, Katharina Wendler, Luigi Delle Site, and Barbara Kirchner. Depolarization of water in protic ionic liquids. *Physical Chemistry Chemical Physics*, 13(33):15083–15093, 2011.
- [38] Urszula Domańska, Izabella Bakala, and Juliusz Pernak. Phase Equilibria of an Ammonium Ionic Liquid with Organic Solvents and Water. *Journal of Chemical & Engineering Data*, 52(1):309–314, 2006.
- [39] U. Domańska and M. Laskowska. Phase equilibria and volumetric properties of (1-ethyl-3-methylimidazolium ethylsulfate+alcohol or water) binary systems. *Journal of Solution Chemistry*, 37(9):1271–1287, 2008.
- [40] Urszula Domańska, Anna Rkawek, and Andrzej Marciniak. Solubility of 1-alkyl-3-ethylimidazolium-based ionic liquids in water and 1-octanol. *Journal of Chemical and Engineering Data*, 53(5):1126–1132, 2008.
- [41] Alexander Stoppa, Johannes Hunger, and Richard Buchner. Conductivities of Binary Mixtures of Ionic Liquids with Polar Solvents Conductivities of Binary Mixtures of Ionic Liquids with Polar Solvents. *Journal of Chemical & Engineering Data*, 54(October 2008):472–479, 2009.
- [42] G. Lakshminarayana, Masayuki Nogami, and I. V. Kityk. Anhydrous Proton Conducting Inorganic–Organic Composite Membranes Based on Tetraethoxysilane/Ethyl-Triethoxysilane/Trimethylphosphate and 1-Butyl-3-methylimidazolium-bis(trifluoromethylsulfonyl)imide. *Journal of The Electrochemical Society*, 157(6):B892–B899, 2010.
- [43] J Le Bideau, L Viau, and A Vioux. Ionogels, ionic liquid based hybrid materials. *Chem Soc Rev*, 40(2):907–925, 2011.

- [44] Anders Riisager, Rasmus Fehrmann, Marco Haumann, and Peter Wasserscheid. Supported ionic liquids: Versatile reaction and separation media. *Topics in Catalysis*, 40:91–102, 2006.
- [45] Marie-alexandra Neouzé, Jean Le Bideau, Philippe Gaveau, Séverine Bellayer, and André Vioux. Ionogels, New Materials Arising from the Confinement of Ionic Liquids within Silica-Derived Networks. *Chemistry of Materials*, 18:3931–3936, 2006.
- [46] Anna Martinelli. Conformational changes and phase behaviour in the protic ionic liquid 1-ethylimidazolium bis(trifluoromethylsulfonyl)imide in the bulk and nano-confined state. *European Journal of Inorganic Chemistry*, 2015(7):1300–1308, 2015.
- [47] Manish Pratap Singh, Rajendra Kumar Singh, and Suresh Chandra. Studies on imidazolium-based ionic liquids having a large anion confined in a nanoporous silica gel matrix. *Journal of Physical Chemistry B*, 115(23):7505–7514, 2011.
- [48] Ronald Göbel, Alwin Friedricha, and Andreas Taubert. Tuning the phase behavior of ionic liquids in organically functionalized silica ionogels. *Dalton transactions*, 39:603–611, 2010.
- [49] Ronald Göbel, Peter Hesemann, Jens Weber, Eléonore Möller, Alwin Friedrich, Sabine Beuermann, and Andreas Taubert. Surprisingly high, bulk liquid-like mobility of silica-confined ionic liquids. *Physical Chemistry Chemical Physics*, 11:3653–3662, 2009.
- [50] Moheb Nayeri, Matthew T. Aronson, Diana Bernin, Bradley F. Chmelka, and Anna Martinelli. Surface effects on the structure and mobility of the ionic liquid C6C1ImTFSI ImTFSI in silica gels. *Soft Matter*, 10(30):5618, 2014.
- [51] Benoit Coasne and Lydie Viau. Loading-Controlled Stiffening in Nanoconfined Ionic Liquids. *The Journal of Physical Chemistry Letters*, 2:1150–1154, 2011.
- [52] P.W. Atkins. *Physical Chemistry*. Oxford, 6 edition, 1999.
- [53] Timothy D W Claridge. *High-resolution NMR techniques in organic chemistry*. Elsevier, 2 edition, 2009.

- [54] Hangchang Chen and Shaw-horng Chen. Diffusion of Crown Ethers in Alcohols. *Journal of Physical Chemistry*, 88:5118–5121, 1984.
- [55] Hiroyuki Tokuda, Kikuko Hayamizu, Kunikazu Ishii, Abu Bin, Hasan Susan, and Masayoshi Watanabe. Physicochemical Properties and Structures of Room Temperature Ionic Liquids . 2 . Variation of Alkyl Chain Length in Imidazolium Cation Physicochemical Properties and Structures of Room Temperature Ionic Liquids . 2 . Variation of Alkyl Chain Length in Im. *Journal of Physical Chemistry B*, 109:6103–6110, 2005.
- [56] Kikuko Hayamizu, Seiji Tsuzuki, Shiro Seki, Kenta Fujii, Masahiko Suenaga, and Yasuhiro Umebayashi. Studies on the translational and rotational motions of ionic liquids composed of N -methyl- N -propyl-pyrrolidinium (P13) cation and bis(trifluoromethanesulfonyl)amide and bis(fluorosulfonyl)amide anions and their binary systems including lithium salts. *Journal of Chemical Physics*, 133(19):194505, 2010.
- [57] Ken Yoshida, Nobuyuki Matubayasi, and Masaru Nakahara. Self-diffusion coefficients for water and organic solvents at high temperatures along the coexistence curve. *Journal of Chemical Physics*, 129(21), 2008.
- [58] N Yaghini, L Nordstierna, and A Martinelli. protic and aprotic imidazolium ionic liquids – an an analysis of self-diffusivity, conductivity, and proton exchange mechanism. *Physical Chemistry Chemical Physics*, 16:9266–9275, 2014.
- [59] Anna Martinelli, Aleksandar Matic, Per Jacobsson, Lars Börjesson, Alessandra Fericola, and Bruno Scrosati. Phase behavior and ionic conductivity in lithium bis(trifluoromethanesulfonyl)imide-doped ionic liquids of the pyrrolidinium cation and bis(trifluoromethanesulfonyl)imide anion. *Journal of Physical Chemistry B*, 113(32):11247–11251, 2009.
- [60] C. A. Angell. Entropy and fragility in supercooling liquids. *J. Res. Natl. Inst. Stand. Technol.*, 102:171, 1997.
- [61] Douglas R. MacFarlane, Maria Forsyth, Ekaterina I. Izgorodina, Andrew P. Abbott, Gary Annat, and Kevin Fraser. On the concept of ionicity in ionic liquids. *Phys. Chem. Chem. Phys.*, 11:4962–4967, 2009.

- [62] Linas Vilčiauskas, Mark E. Tuckerman, Gabriel Bester, Stephen J. Paddison, and Klaus-Dieter Kreuer. The mechanism of proton conduction in phosphoric acid. *Nature Chemistry*, 4(6):461–466, 2012.
- [63] K. D. Kreuer, S. J. Paddison, E. Spohr, and M. Schuster. Transport in proton conductors for fuel cell applications: simulation, elementary reactions and phenomenology. *Chemical Reviews*, 104:4637–4678, 2004.
- [64] John W Blanchard, Jean-philippe Belin, Todd M Alam, Jeffery L Yarger, and Gregory P Holland. NMR Determination of the Diffusion Mechanisms in. *The Journal of Physical Chemistry Letters*, 2:1077–1081, 2011.
- [65] Tatsiana Burankova, Rolf Hempelmann, Verlaïne Fossog, Jacques Ollivier, Tilo Seydel, and Jan P. Embs. Proton Diffusivity in the Protic Ionic Liquid Triethylammonium Triflate Probed by Quasielastic Neutron Scattering. *Journal of Physical Chemistry B*, 119(33):10643–10651, 2015.
- [66] Megan L. Hoarfrost, Madhusudan Tyagi, Rachel A. Segalman, and Jeffrey A. Reimer. Proton hopping and long-range transport in the protic ionic liquid [Im][TFSI], probed by pulsed-field gradient NMR and quasi-elastic neutron scattering. *Journal of Physical Chemistry B*, 116(28):8201–8209, 2012.
- [67] Linas Vilčiauskas, Mark E. Tuckerman, Jan P. Melchior, Gabriel Bester, and Klaus Dieter Kreuer. First principles molecular dynamics study of proton dynamics and transport in phosphoric acid/imidazole (2:1) system. *Solid State Ionics*, 252:34–39, 2013.
- [68] Ala’a K. Abdul-Sada, Anthony M. Greenway, Peter B. Hitchcock, Thamer J. Mohammed, Kenneth R. Seddon, and Jalal a. Zora. Upon the structure of room temperature halogenoaluminate ionic liquids. *Journal of the Chemical Society, Chemical Communications*, pages 1753–1754, 1986.
- [69] Ralf Ludwig. The effect of dispersion forces on the interaction energies and far infrared spectra of protic ionic liquids. *Physical Chemistry Chemical Physics*, 17(21):13790–3, 2015.

- [70] Koichi Fumino, Verlainé Fossog, Peter Stange, Dietmar Paschek, Rolf Hempelmann, and Ralf Ludwig. Controlling the subtle energy balance in protic ionic liquids: Dispersion forces compete with hydrogen bonds. *Angewandte Chemie - International Edition*, 54(9):2792–2795, 2015.
- [71] Koichi Fumino, Alexander Wulf, and Ralf Ludwig. Strong, localized, and directional hydrogen bonds fluidize ionic liquids. *Angewandte Chemie - International Edition*, 47(45):8731–8734, 2008.
- [72] K. Fumino, T. Peppel, M. Geppert-Rybczynska, D. H. Zaitsau, J. K. Lehmann, S. P. Verevkin, M. Köckerling, and R Ludwig. The influence of hydrogen bonding on the physical properties of ionic liquids. *Physical Chemistry Chemical Physics*, 13:14064–14075, 2011.
- [73] Stefan Grimme, Waldemar Hujoa, and Barbara Kirchner. Performance of dispersion-corrected density functional theory for the interactions in ionic liquids. *Physical Chemistry Chemical Physics*, 14:4875–4883, 2012.
- [74] Gary Annat, Douglas R Macfarlane, and Maria Forsyth. Transport properties in ionic liquids and ionic liquid mixtures: the challenges of NMR pulsed field gradient diffusion measurements. *The Journal of Physical Chemistry B*, 111(30):9018–9024, 2007.
- [75] Peter J. Larkin. *IR and Raman Spectroscopy- Principles and Spectral Interpretation*. Elsevier, 2011.
- [76] Seiji Tsuzuki, Seiji Tsuzuki, Wataru Shinoda, Wataru Shinoda, Hiroaki Saito, Hiroaki Saito, Masuhiro Mikami, Masuhiro Mikami, Hiroyuki Tokuda, Hiroyuki Tokuda, Masayoshi Watanabe, and Masayoshi Watanabe. Molecular Dynamics Simulations of Ionic Liquids: Cation and Anion Dependence of Self-Diffusion Coefficients of Ions. *Journal of Physical Chemistry B*, pages 10641–10649, 2009.
- [77] Amrish Menjoge, Janeille Dixon, Joan F Brennecke, Edward J Maginn, and Sergey Vasenkov. Influence of water on diffusion in imidazolium-based ionic liquids: a pulsed field gradient NMR study. *The Journal of Physical Chemistry B*, 113:6353–6359, 2009.

- [78] Manish S Kelkar, Wei Shi, and Edward J Maginn. Determining the Accuracy of Classical Force Fields for Ionic Liquids : Atomistic Simulation of the Thermodynamic and Transport Properties of 1-Ethyl-3-methylimidazolium Ethylsulfate ([emim][EtSO₄]) and Its Mixtures with Water. *Ind. Eng. Chem. Res.*, 47(23):9115–9126, 2008.
- [79] Md. Abu Bin Hasan Susan, Akihiro Noda, Shigenori Mitsushima, and Masayoshi Watanabe. Brønsted acid-base ionic liquids and their use as new materials for anhydrous proton conductors. *Chemical Communications*, 8(8):938–939, 2003.
- [80] L. M. Varela, J. Carrete, M. Garcia, L. J. Gallego, M. Turmine, E. Rilo, and O. Cabeza. Pseudolattice theory of charge transport in ionic solutions: Corresponding states law for the electric conductivity. *Fluid Phase Equilibria*, 298(2):280–286, 2010.
- [81] E. Rilo, J. Vila, S. Garcia-Garabal, L. M. Varela, and O. Cabeza. Electrical conductivity of seven binary systems containing 1-ethyl-3-methyl imidazolium alkyl sulfate ionic liquids with water or ethanol at four temperatures. *Journal of Physical Chemistry B*, 117(5):1411–1418, 2013.
- [82] L. Cammarata, S. G. Kazarian, P. a. Salter, and T. Welton. Molecular states of water in room temperature ionic liquids. *Physical Chemistry Chemical Physics*, 3(23):5192–5200, 2001.
- [83] B Kumar, T Singh, K S Rao, A Pal, and A Kumar. Thermodynamic and spectroscopic studies on binary mixtures ionic liquids in ethylene glycol. *Journal of Chemical Thermodynamics*, 44(1):121–127, 2012.
- [84] Tejwant Singh, K. Srinivasa Rao, and Arvind Kumar. Polarity behaviour and specific interactions of imidazolium-based ionic liquids in ethylene glycol. *ChemPhysChem*, 12(4):836–845, 2011.
- [85] James Keeler. *Understanding NMR Spectroscopy*. Wiley, 2nd edition, 2010.
- [86] Meriem Anouti, Johan Jacquemin, and Patrice Porion. Transport properties investigation of aqueous protic ionic liquid solutions through conductivity, viscosity, and NMR self-diffusion measurements. *Journal of Physical Chemistry B*, 116(14):4228–4238, 2012.

- [87] Stephen K Davidowski, Forrest Thompson, Wei Huang, Mohammad Hasani, Samrat A. Amin, Charles Austen Angell, and Jeffrey L. Yarger. NMR Characterization of Ionicity and Transport Properties for a Series of Diethylmethylamine Based Protic Ionic Liquids. *The Journal of Physical Chemistry B*, 120:4279–4285, 2016.
- [88] O’Hyre and P Rayan. *Fuel cell fundamentals*. Wiley, 2nd edition, 2009.
- [89] Supramaniam Srinivasan. *Fuel Cells: From Fundamentals to Applications*. Springer, 2006.
- [90] Scherer. *Fuel cell I*. Springer, 2008.

